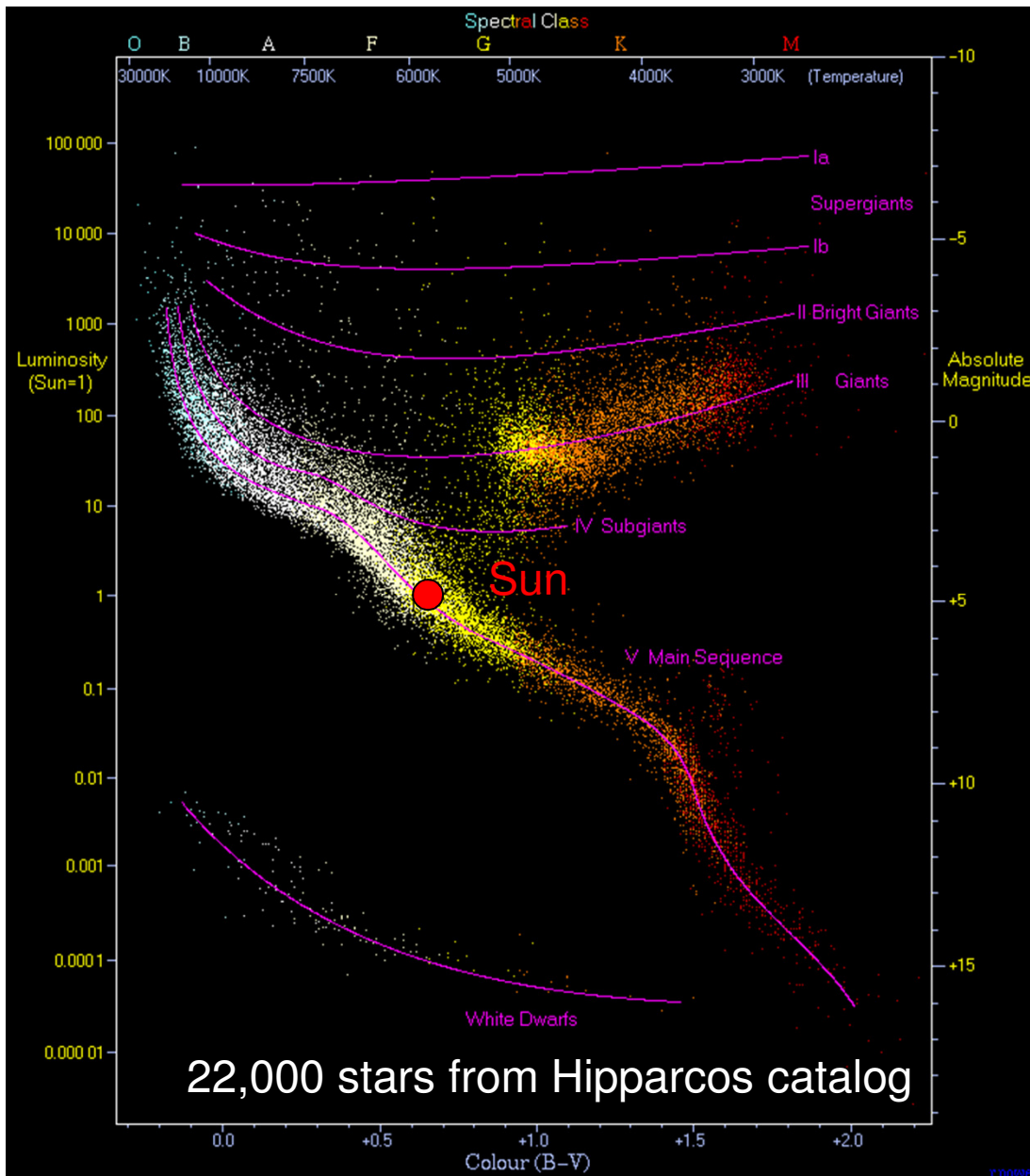


2. The Sun as a star

General properties, place in the Hertzsprung-Russell diagram. Distance, mass, radius, luminosity, composition, age, evolution, spectral energy distribution.

General Properties of the Sun. Hertzsprung-Russel Diagram.



- In 1911-13, Ejnar Hertzsprung and Henry Norris Russell independently developed H-R diagram
 - Horizontal axis - spectral type (or, equivalently, color index or surface temperature)
 - Vertical axis - absolute magnitude (or luminosity)
- Data points define definite regions, suggesting common relationship exists for stars composing region. Each region represents stage in evolution of stars.
- The place of a star on the H-R diagram also tells us about its radius, energy generation and transport, periods and growth rates of pulsations, rotation rate, stellar activity, X-ray coronas, etc.
- Sun is G2 main-sequence star. Lies roughly in middle of diagram among what are referred to as yellow dwarfs.

Overall properties

Age	4.5×10^9 years	$10^{10.65}$ years
Mass (M_{\odot})	1.99×10^{33} g	$10^{33.30}$ g
Radius (R_{\odot})	6.96×10^{10} cm	$10^{10.84}$ cm
Mean density	1.4 g cm^{-3}	$10^{0.15} \text{ g cm}^{-3}$
Mean distance from Earth (AU)	1.5×10^{13} cm	$10^{13.84}$ cm
Surface gravity (g_{\odot})	$2.74 \times 10^4 \text{ cm s}^{-2}$	$10^{4.44} \text{ cm s}^{-2}$
Escape velocity	$6.17 \times 10^7 \text{ cm s}^{-1}$	$10^{7.79} \text{ cm s}^{-1}$
Luminosity (L_{\odot})	$3.83 \times 10^{33} \text{ erg s}^{-1}$	$10^{33.59} \text{ erg s}^{-1}$
Equatorial rotation period	26 days	$10^{6.35}$ s
Angular momentum	$1.7 \times 10^{48} \text{ g cm}^2 \text{ s}^{-1}$	$10^{48.23} \text{ g cm}^2 \text{ s}^{-1}$
Mass loss rate	10^{12} g s^{-1}	
Effective temperature (T_e)	5772 K	$10^{3.76}$ K
1 arc sec	726 km	$10^{7.86}$ cm

Sun's age

The age of the Sun is estimated from meteorites, the oldest bodies in the solar system. Their age is determined from the decay of radioactive isotopes, such as ^{87}Rb (Rubidium) which has a half-life of 4.8×10^{10} years. It decays into stable isotope Strontium (^{87}Sr).

$$^{87}\text{Sr}_{\text{now}} = ^{87}\text{Sr}_{\text{original}} + (^{87}\text{Rb}_{\text{original}} - ^{87}\text{Rb}_{\text{now}})$$

$$^{87}\text{Rb}_{\text{original}} = ^{87}\text{Rb}_{\text{now}} \times e^{\lambda t}$$

Radioactive decay

$$^{87}\text{Sr}_{\text{now}} = ^{87}\text{Sr}_{\text{original}} + ^{87}\text{Rb}_{\text{now}} \times (e^{\lambda t} - 1).$$

$$\frac{^{87}\text{Sr}_{\text{now}}}{^{86}\text{Sr}} = \frac{^{87}\text{Sr}_{\text{original}}}{^{86}\text{Sr}} + \frac{^{87}\text{Rb}_{\text{now}}}{^{86}\text{Sr}} \times (e^{\lambda t} - 1).$$

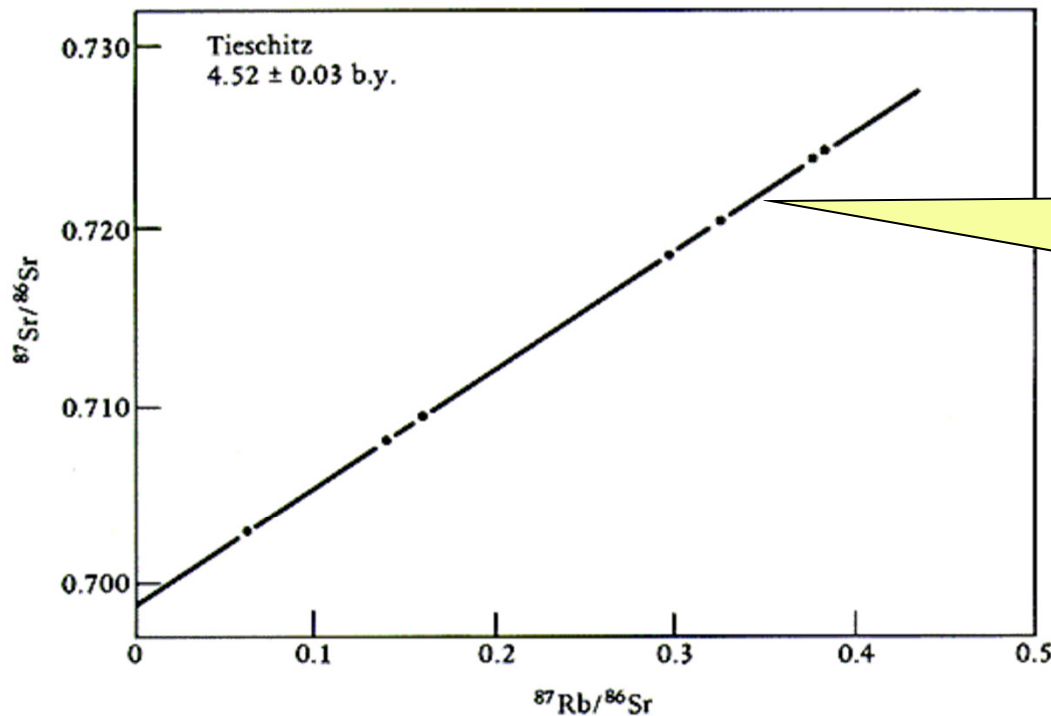
Does not change over time

Measured by mass spectrometer

$$\frac{{}^{87}\text{Sr}_{\text{now}}}{{}^{86}\text{Sr}} = \frac{{}^{87}\text{Sr}_{\text{original}}}{{}^{86}\text{Sr}} + \frac{{}^{87}\text{Rb}_{\text{now}}}{{}^{86}\text{Sr}} \times (e^{\lambda t} - 1).$$

Note that this is the equation of a line in the form

$$y = b + x \cdot m \quad m = (e^{\lambda t} - 1)$$



The age is determined from the slope

Precise measurement of radioactive isotopes provides a way to determine the age of a meteorite. In the method illustrated here, a radioactive isotope of rubidium (${}^{87}\text{Rb}$) decays to a stable isotope of strontium (${}^{87}\text{Sr}$), which mixes with already existing strontium isotopes (${}^{87}\text{Sr}$ and ${}^{86}\text{Sr}$). The individual data points in this diagram represent minerals separated from the Tieschitz (Czechoslovakia) chondrite. The age of the meteorite (4.52 billion years) is calculated from the slope of the diagonal line, which steepens with increasing time.

New solar parameters adopted by the International Astronomical Union (2015)

that the IAU (2015) System of Nominal Solar and Planetary Conversion Constants be adopted as listed below:

SOLAR CONVERSION CONSTANTS		
$1R_{\odot}^N$	=	$6.957 \times 10^8 \text{ m}$
$1S_{\odot}^N$	=	1361 W m^{-2}
$1L_{\odot}^N$	=	$3.828 \times 10^{26} \text{ W}$
$1T_{\text{eff}\odot}^N$	=	5772 K
$1(GM)_{\odot}^N$	=	$1.327\,124\,4 \times 10^{20} \text{ m}^3 \text{ s}^{-2}$

Distance - I

Until recently distances in the solar system were measured by triangulation. More accurate results are obtained by measuring radar echos.

In principle, a single measurement of a linear distance between two bodies of the solar system is sufficient to derive all distances between the planets and the Sun.

This is because of Kepler's third law which relates semi-major axes a_i and periods T_i for a body m :

$$\frac{a^3}{T^2} = \frac{GM_{\odot}}{4\pi^2} (1 + m/M_{\odot}).$$

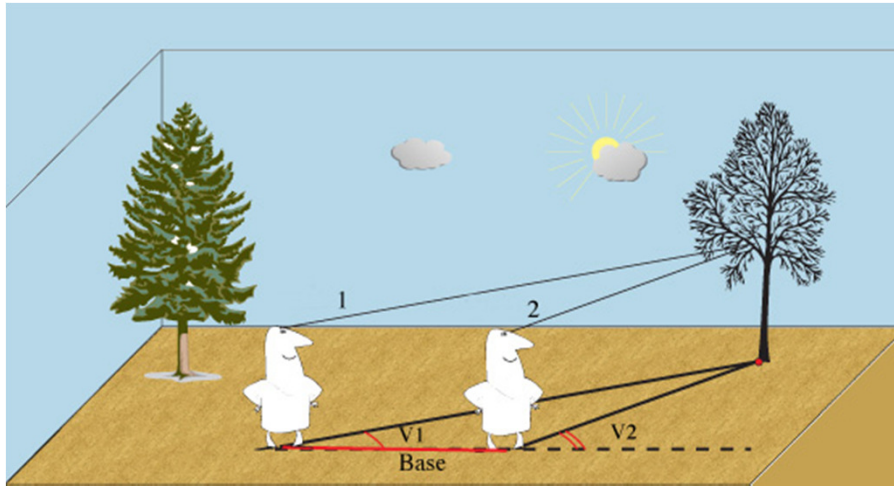
The ratios of the semi-major axes of two bodies is:

$$\left(\frac{a_1}{a_2}\right)^3 = \left(\frac{T_1}{T_2}\right)^2 \frac{1 + m_1/M_{\odot}}{1 + m_2/M_{\odot}}.$$

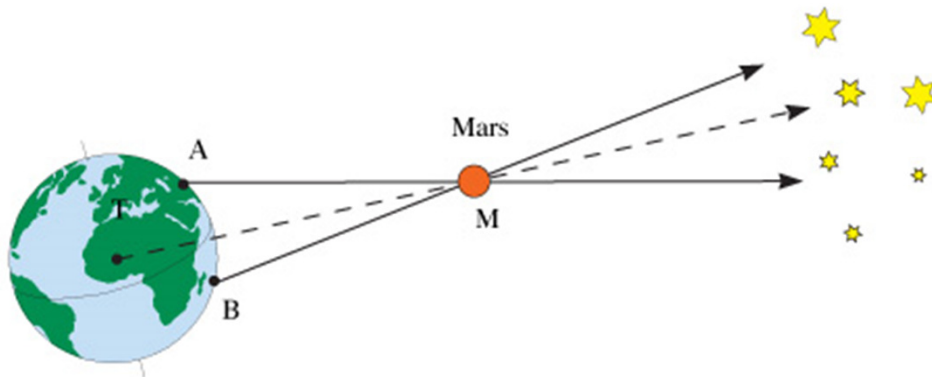
Masses m_1 and m_2 are determined from the mutual perturbations of planetary orbits.

The Sun is not used directly to determine the distance to the Sun, the astronomical unit (AU).

Distance - II



Triangulation

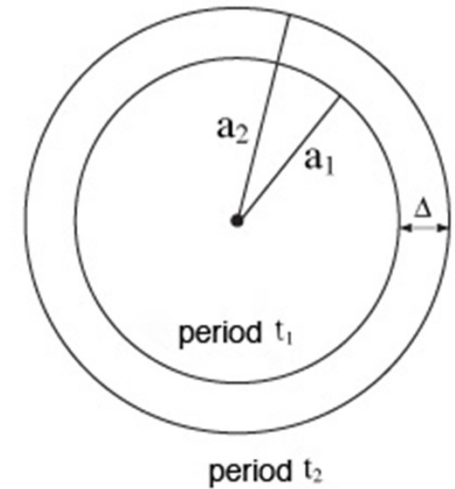


Kepler's law

$$\frac{a_1^3}{t_1^2} = \frac{a_2^3}{t_2^2}$$

$$a_1 = a_2 - \Delta$$

➔ a_1 et a_2



Measure the distance between the planets, Δ , the orbital periods, t_1 and t_2 , and then calculate their distances to the Sun, a_1 and a_2 .

Distance - III

The light time for 1 AU is:

$$\tau_A = 499.004782 \pm 0.000006 \text{ s.}$$

The speed of light by definition (since 1983) is

$$c = 299792458 \text{ m s}^{-1}.$$

Then, $1AU = 149597880 \pm 2 \text{ km.}$

The major semi-axis for the Earth is

$$a = 1.000000036 \text{ AU} \approx 1.496 \times 10^{13} \text{ cm.}$$

Linear distances on the Sun are measured in arc sec:

$$1'' \approx 726 \text{ km at the disk center.}$$

The Sun's angular size varies from 31' 27.7" to 32' 31.9" during the course of a year because the distance changes from $1.471 \times 10^{11} \text{ m}$ in January to $1.521 \times 10^{11} \text{ m}$ in July.

1 arcsec varies from 710 km to 734 km.

The Solar Mass

Once distances are known the Sun's mass is determined from Kepler's law. Only the product, GM_{\odot} , is determined with high precision:

$$GM_{\odot} = (1.32712438 \pm 0.000000005) \times 10^{26} \text{ cm}^3 \text{ s}^{-2}.$$

The gravitation constant is determined in laboratory measurements:

$$G = (6.672 \pm 0.004) \times 10^{-8} \text{ cm}^3 \text{ g}^{-1} \text{ s}^{-2}.$$

Therefore,

$$M_{\odot} = (1.9891 \pm 0.0012) \times 10^{33} \text{ g}.$$

Mass loss due to the energy radiated into space:

$$dM_{\odot}/dt = L_{\odot}/c^2 \approx 4 \times 10^{12} \text{ g s}^{-1}.$$

Mass loss due to the solar wind: $\approx 10^{12} \text{ g s}^{-1}$.

The total loss during the Sun's life of $\approx 1.5 \times 10^{17} \text{ s}$: $\approx 7.5 \times 10^{29} \text{ g}$ (0.04%).

Sun's rotation axis is inclined by 7.23 degrees to the ecliptic

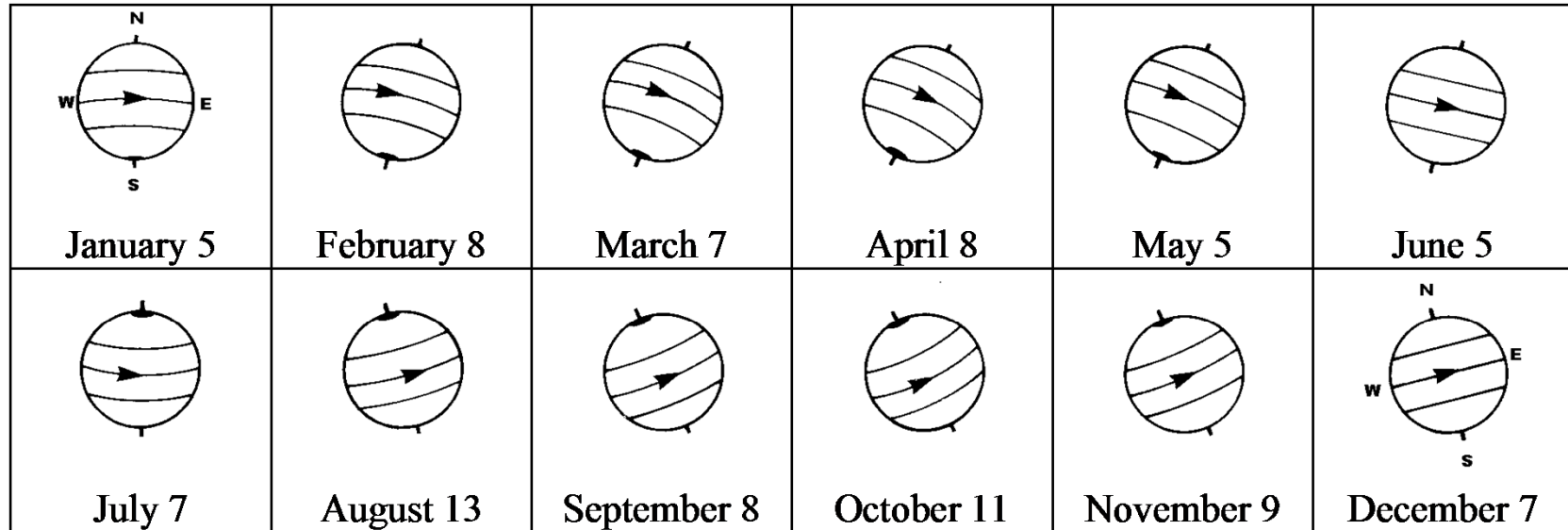
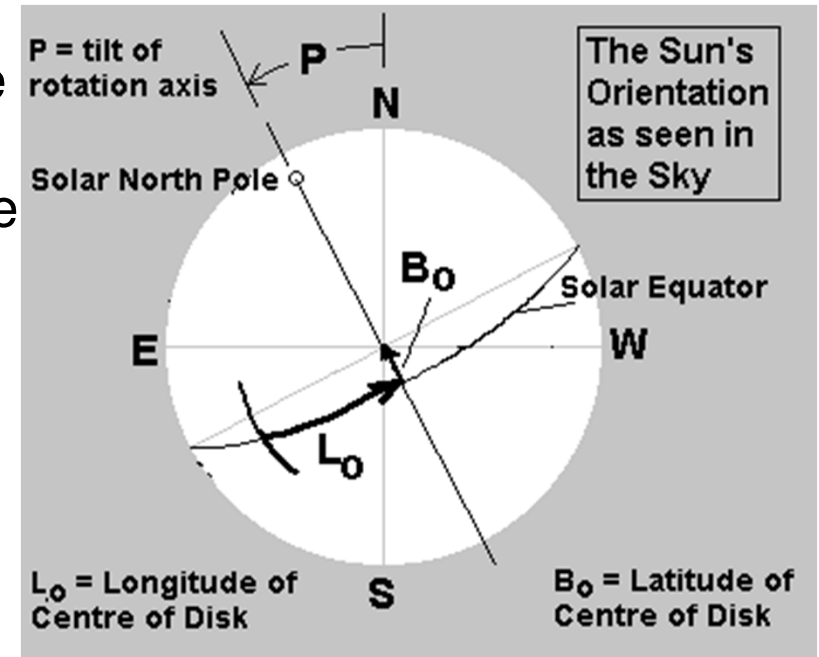


Figure : Due to the Earth revolution and axis inclination, the position angle of the Sun's axis is varying all along the sidereal year. The value of this angle is near zero around Earth perihelion and aphelion. The distance of the Sun's rotational poles from the limb has been exaggerated: at maximum the shift reaches 7° . We can only see the sunspots' paths as straight lines in early June and December.

Solar coordinates

- **P-angle (or P):** The position angle between the geocentric north pole and the solar rotational north pole measured eastward from geocentric north. The range in P is +/- 26.31 degrees.
- **B₀:** Heliographic latitude of the central point of the solar disk; also called the B-angle. The range of B₀ is +/- 7.23 degrees, correcting for the tilt of the ecliptic with respect to the solar equatorial plane.
- **L₀:** Heliographic longitude of the central point of the solar disk. The longitude value is determined with reference to a system of fixed longitudes rotating on the Sun at a rate of 13.2 degrees/day (the mean rate of rotation observed from central meridian transits of sunspots). The standard meridian on the Sun is defined to be the meridian that passed through the Sun's equator on 1 January 1854 at 1200 UTC and is calculated for the present day by assuming a uniform sidereal period of rotation of 25.38 days. (Carrington longitude).



The Solar Radius

The angular diameter is defined as the angular distance between the inflection points of the intensity profile at two opposite limbs. It is measured photoelectrically.

Results for the solar radius:

apparent angular	apparent linear	photospheric($\tau = 1$)
¹ $960''.01 \pm 0''.1$	$(6.9626 \pm 0.0007) \times 10^{10}$ cm	6.960×10^{10} cm
² $959''.68 \pm 0''.01$	$(6.9602 \pm 0.00007) \times 10^{10}$ cm	6.955×10^{10} cm

¹ Wittman, A. 1977, *Astron. Astrophys.*, 61, 255

² Brown, T.M. & Christensen-Dalsgaard, J. 1998, *ApJ*, 500, L195.

The current reference value is: $(6.9566 \pm 0.0001) \times 10^{10}$ cm =
 695.66 ± 0.01 Mm.

Determination of the seismic radius

THE ASTROPHYSICAL JOURNAL, 489:L197–L200, 1997 November 10
© 1997. The American Astronomical Society. All rights reserved. Printed in U.S.A.

DETERMINATION OF THE SUN'S SEISMIC RADIUS FROM THE *SOHO* MICHELSON DOPPLER IMAGER

J. SCHOU AND A. G. KOSOVICHEV

W. W. Hansen Experimental Physics Laboratory, Stanford University, Stanford, CA 94305-4085; akosovichev@solar.stanford.edu, jschou@solar.stanford.edu

P. R. GOODE

Department of Physics, New Jersey Institute of Technology, Newark, NJ 07102

AND

W. A. DZIEMBOWSKI

N. Copernicus Astronomical Center, Bartycka 18, 00-716 Warsaw, Poland

Received 1997 May 28; accepted 1997 September 8; published 1997 October 13

ABSTRACT

Dopplergrams from the Michelson Doppler Imager (MDI) instrument on board the *SOHO* spacecraft have been used to accurately measure frequencies of the Sun's fundamental (f) mode in the medium angular degree range, $l = 88$ – 250 . The comparison of these frequencies with the corresponding frequencies of the standard solar models suggests that the apparent photospheric solar radius (695.99 Mm) used to calibrate the models should be reduced by approximately 0.3 Mm. The precise value of the seismologically determined solar radius depends on the description of the subsurface layer of superadiabatic convection. The discrepancy between the “seismic” and apparent photospheric radii is not explained by the known systematic errors in the helioseismic and photospheric measurements. If confirmed, this discrepancy represents an interesting new challenge to theories of solar convection and solar modeling.

Subject headings: Sun: evolution — Sun: fundamental parameters — Sun: interior — Sun: oscillations

Helioseismic estimate of the solar radius

Helioseismic estimate of the solar radius from f-mode frequencies: $(6.9568 \pm 0.0003) \times 10^{10}$ cm (Schou, J. et al., 1997, ApJ, 489, L197).

The frequencies of the f mode (surface gravity wave) depend only on the horizontal wavenumber $k = \sqrt{l(l+1)}/R_{\odot}$ (l is the mode angular degree) and surface gravity $g = GM_{\odot}/R_{\odot}^2$:

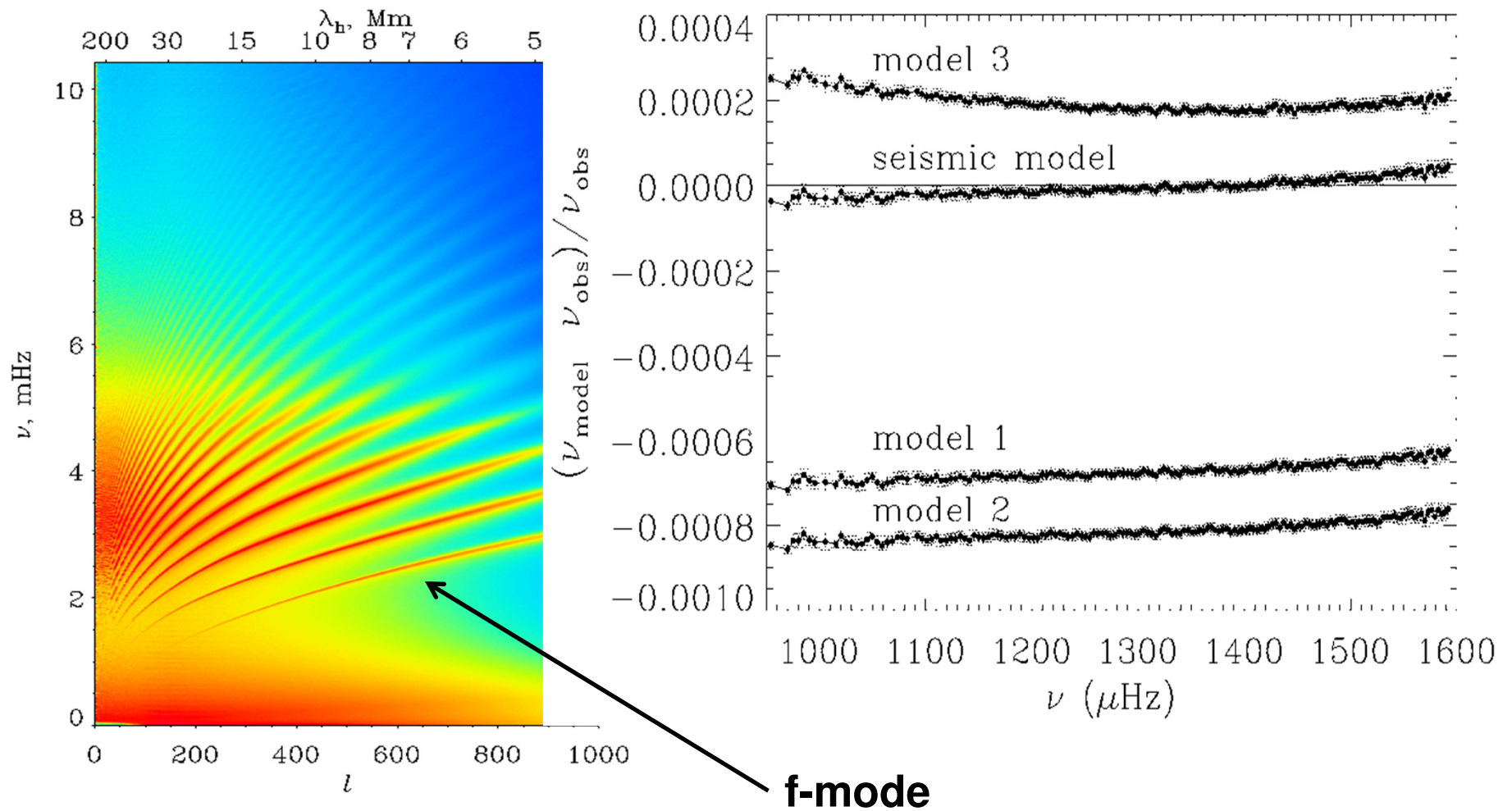
$$\omega = \sqrt{gk} = \sqrt{GM_{\odot}[l(l+1)]^{1/2}/R_{\odot}^3}.$$

This allows us to estimate R_{\odot} from the wave dispersion relation, $\omega(l)$, and GM_{\odot} .

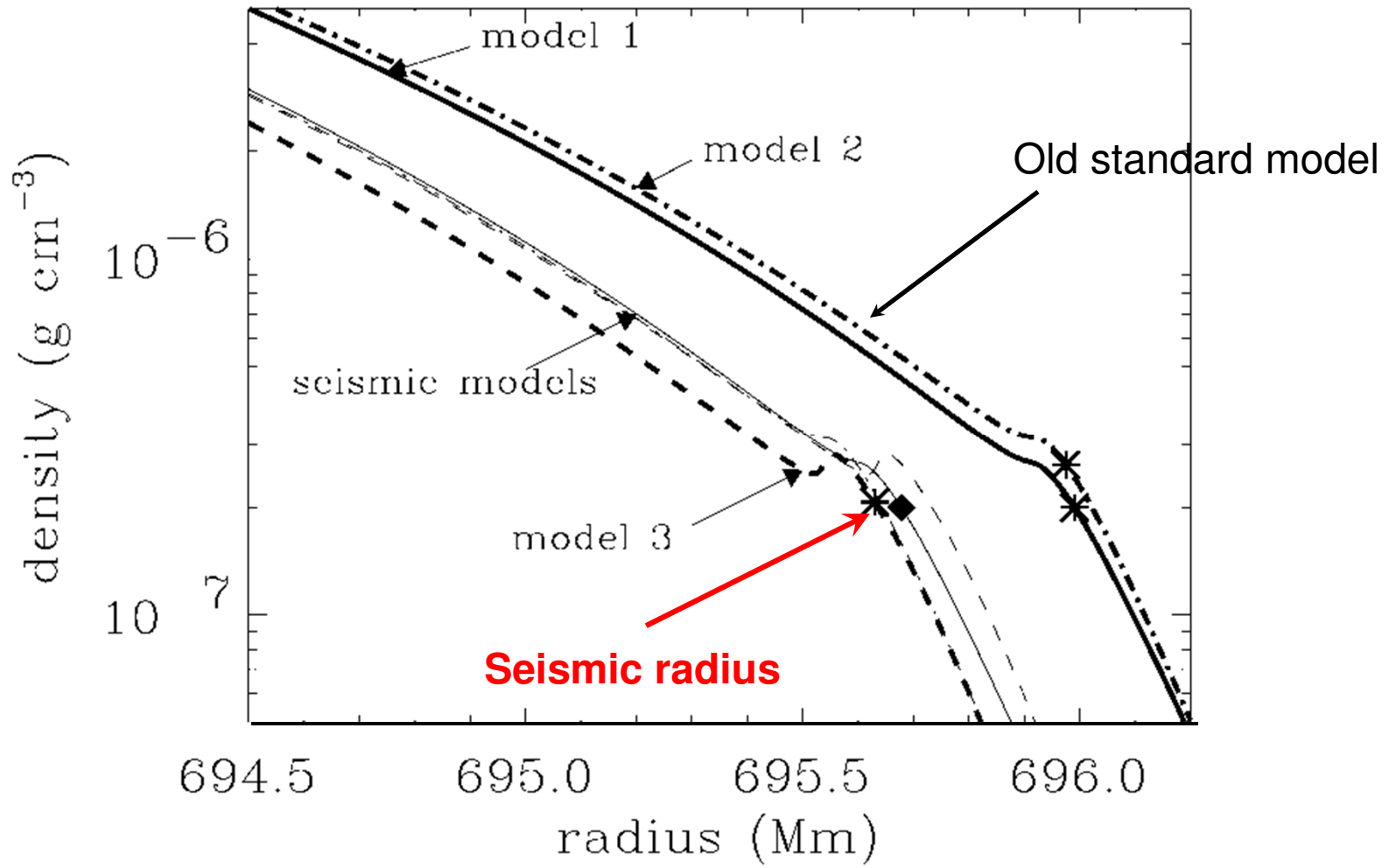
The evolutionary change of the solar radius: $dR_{\odot}/dt \approx 2.4$ cm/year.

There is evidence that the solar radius changes by 1-2 km with the solar activity cycle.

Measurements of f-mode frequencies and comparison with solar models



Calibration of solar models to match the helioseismology data



SOLVING THE DISCREPANCY BETWEEN THE SEISMIC AND PHOTOSPHERIC SOLAR RADIUS

M. HABERREITER AND W. SCHMUTZ

Physikalisch-Meteorologisches Observatorium Davos, World Radiation Center, Dorfstrasse 33, 7260 Davos, Switzerland; margit.haberreiter@pmodwrc.ch

AND

A. G. KOSOVICHEV

W. W. Hansen Experimental Physics Laboratory, Stanford University, Stanford, CA 94305-4085; sasha@quake.stanford.edu

Received 2007 November 14; accepted 2008 January 14; published 2008 January 25

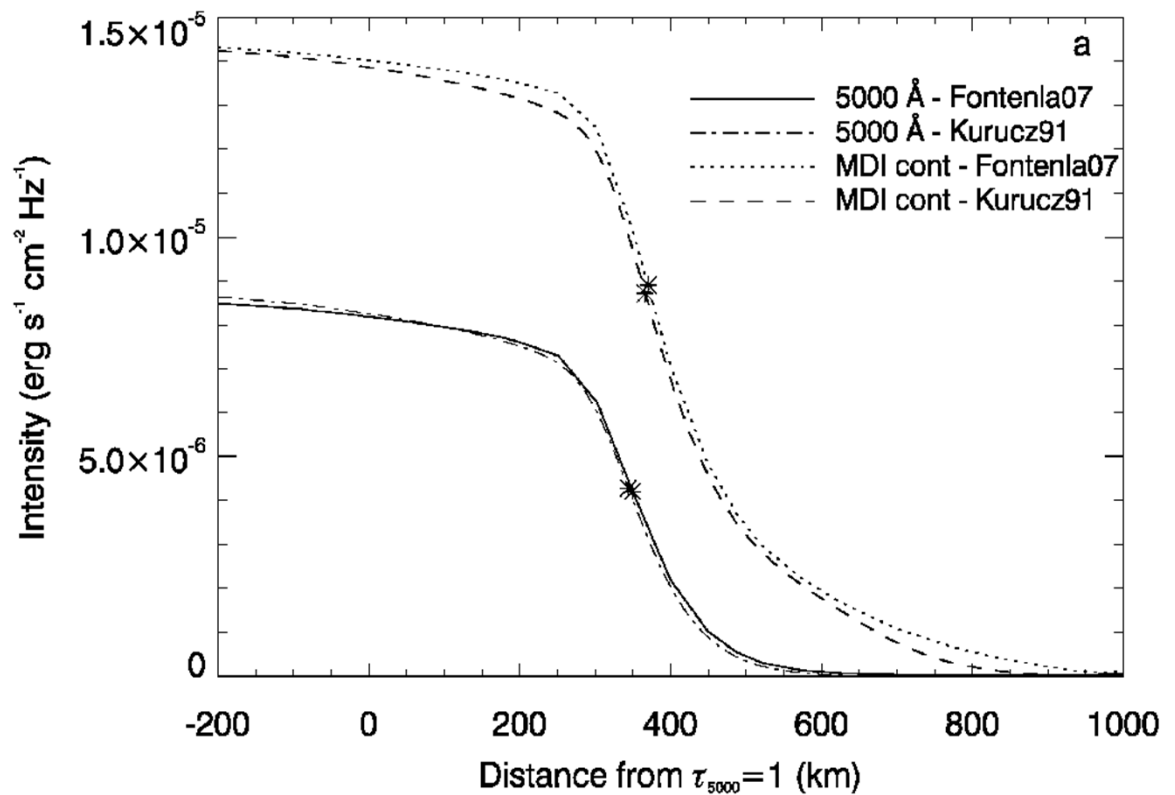
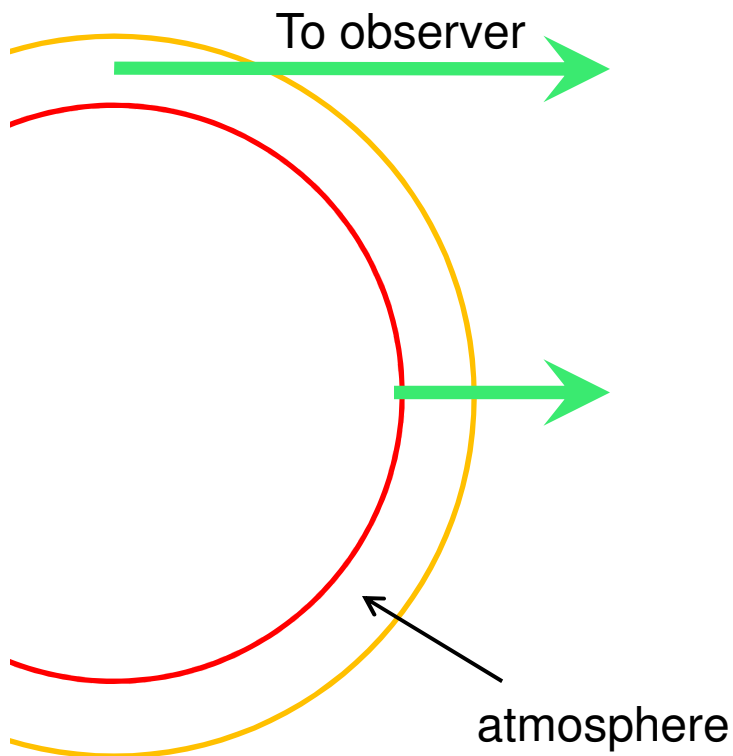
ABSTRACT

Two methods are used to observationally determine the solar radius: One is the observation of the intensity profile at the limb; the other one uses f -mode frequencies to derive a “seismic” solar radius which is then corrected to optical depth unity. The two methods are inconsistent and lead to a difference in the solar radius of ~ 0.3 Mm. Because of the geometrical extension of the solar photosphere and the increased path lengths of tangential rays the Sun appears to be larger to an observer who measures the extent of the solar disk. Based on radiative transfer calculations we show that this discrepancy can be explained by the difference between the height at disk center where $\tau_{5000} = 1$ ($\tau_{\text{Ross}} = 2/3$) and the inflection point of the intensity profile on the limb. We calculate the intensity profile of the limb for the MDI continuum and the continuum at 5000 \AA for two atmosphere structures and compare the position of the inflection points with the radius at $\tau_{5000} = 1$ ($\tau_{\text{Ross}} = 2/3$). The calculated difference between the seismic radius and the inflection point is 0.347 ± 0.006 Mm with respect to $\tau_{5000} = 1$, and 0.333 ± 0.008 Mm with respect to $\tau_{\text{Ross}} = 2/3$. We conclude that the standard solar radius in evolutionary models has to be lowered by 0.333 ± 0.008 Mm and is 695.66 Mm. Furthermore, this correction reconciles inflection point measurements and the seismic radii within the uncertainties.

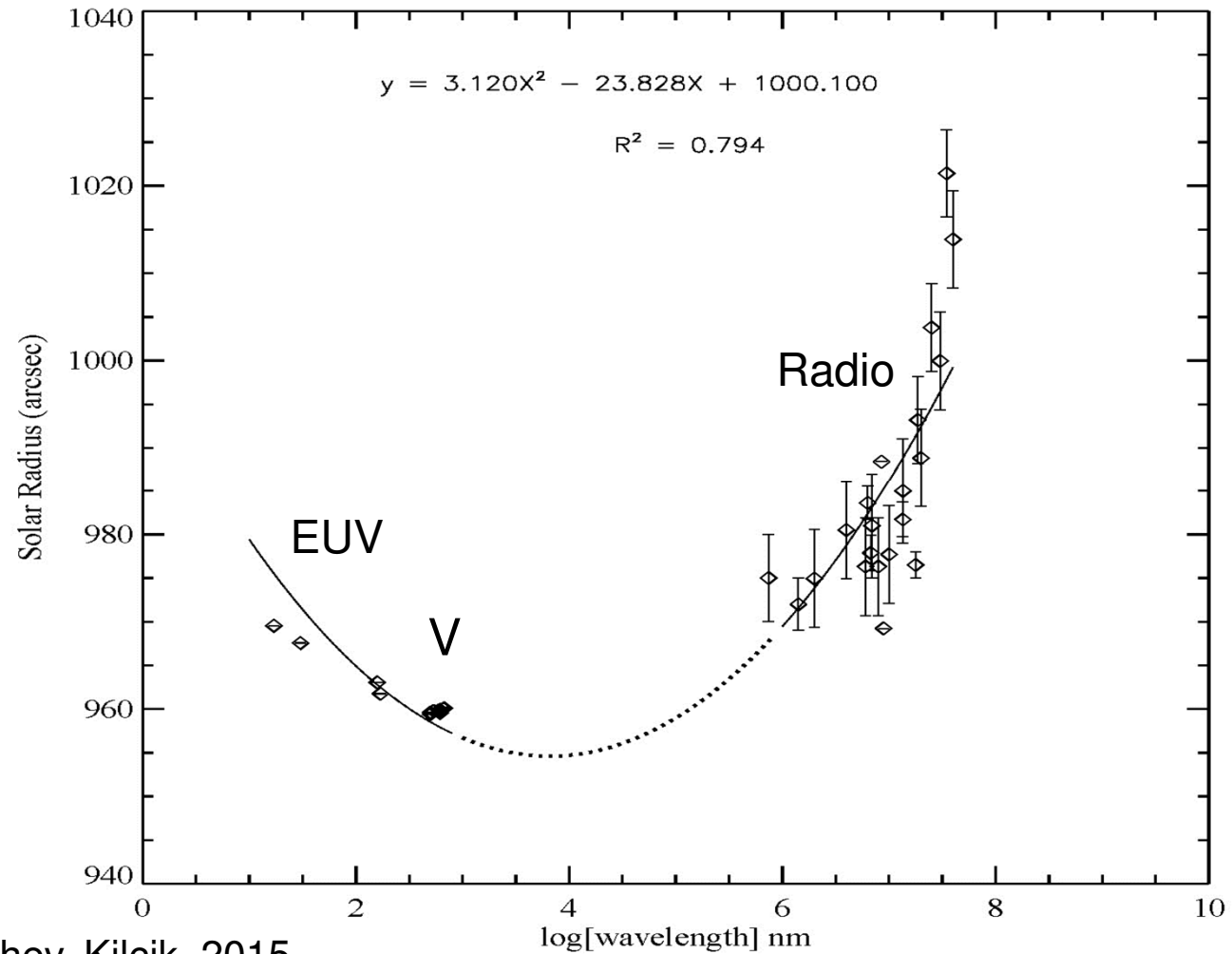
Subject headings: astrometry — radiative transfer — Sun: fundamental parameters — Sun: photosphere

Radiative transfer calculations to determine the precise surface location

At the limb we see higher layers of the solar atmosphere because of the higher optical depth. The reference wavelength is 5000Å.



The apparent solar radius depends on wavelength (the standard value is for 5,000Å=500nm)



Oblateness

Oblateness is defined as $(R_{\text{equator}} - R_{\text{pole}})/R_{\odot} = \Delta R/R_{\odot}$

Origin: rotation + magnetic fields (?).

Measurements:

$$R_{\text{surf}}(\theta) = R_{\odot} \left[1 + \sum_{n=2}^{\text{even } n} r_n P_n(\cos \theta) \right],$$

where P_n are Legendre polynomials.

	r_2	r_4
Solar Disk		
Sextant ¹	$(-5.810 \pm 0.400) \times 10^{-6}$	$(-4.17 \pm 4.59) \times 10^{-7}$
SOHO/MDI ²	$(-5.329 \pm 0.452) \times 10^{-6}$	$(-5.53 \pm 0.40) \times 10^{-7}$ (1996) $(-1.41 \pm 0.55) \times 10^{-7}$ (1997)

¹ Lydon, T.J. & Sofia, S. 1996, Phys.Rev.Lett., 76, 177.

² Kuhn, J. et al. 1998, Nature, 392, 155.

Quadrupole moment

The gravitational potential:

$$\Phi(r, \theta) = -\frac{GM_{\odot}}{r} \left[1 - J_2 \left(\frac{R_{\odot}}{r} \right)^2 P_2(\theta) \right],$$

where J_2 is the quadrupole moment.

From the equation of hydrostatic equilibrium:

$$J_2 = \frac{\Omega^2 R_{\odot}}{3g} - r_2,$$

where Ω is the Sun's angular velocity.

The first term is almost equal to r_2 :

$$\frac{\Omega^2 R_{\odot}}{3g} \approx -5.625 \times 10^{-6}.$$

Therefore, $J_2 = (1.84 \pm 4.0) \times 10^{-7}$.

If general relativity describes the advance of perihelion of Mercury, then 42.98 ± 0.04 acrsec/century corresponds to a quadrupole moment $(2.3 \pm 3.1) \times 10^{-7}$.

Composition

The approximate fraction of the mass of the plasma near the surface of the Sun:

<u>Element</u>	<u>abundance</u>
H (hydrogen)	0.735 – 0.75
He (helium)	0.248 – 0.25
Li (lithium)	1.55×10^{-9}
Be (beryllium)	1.41×10^{-11}
B (boron)	2.00×10^{-10}
C (carbon)	3.72×10^{-4}
N (nitrogen)	1.15×10^{-4}
O (oxygen)	6.76×10^{-4}

Solar composition

- **Solar (stellar) composition** is determined by the fractional percentage of hydrogen, **X**, helium, **Y**, and the heavier elements, **Z**:
- **X+Y+Z=1**
- **X=m_H/M** (M is the total mass)
- **Y=m_{He}/M**
- **Z=1-X-Y**

Canonical values:

Hydrogen mass fraction $X_{\text{sun}} = 0.73$

Helium mass fraction $Y_{\text{sun}} = 0.25$

Heavy elements $Z_{\text{sun}} = 0.02$

Logarithmic abundances are defined relatively to the number density of hydrogen:

$$\log \epsilon_X = \log(N_X/N_H) + 12$$

N_X – number density of element X

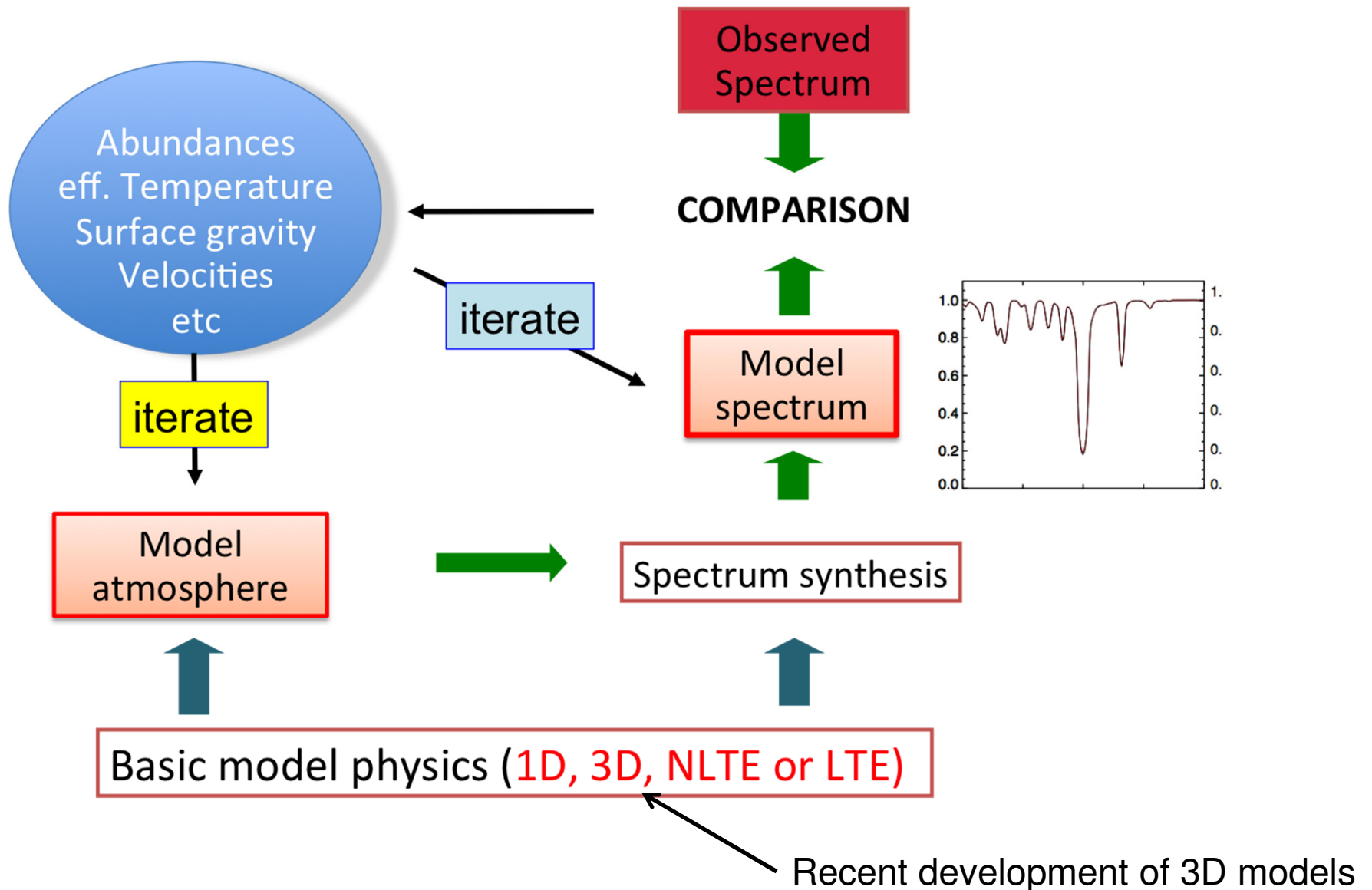
N_H – number density of hydrogen H

Stellar “metallicity” is defined relative to the Sun [Fe/H]:

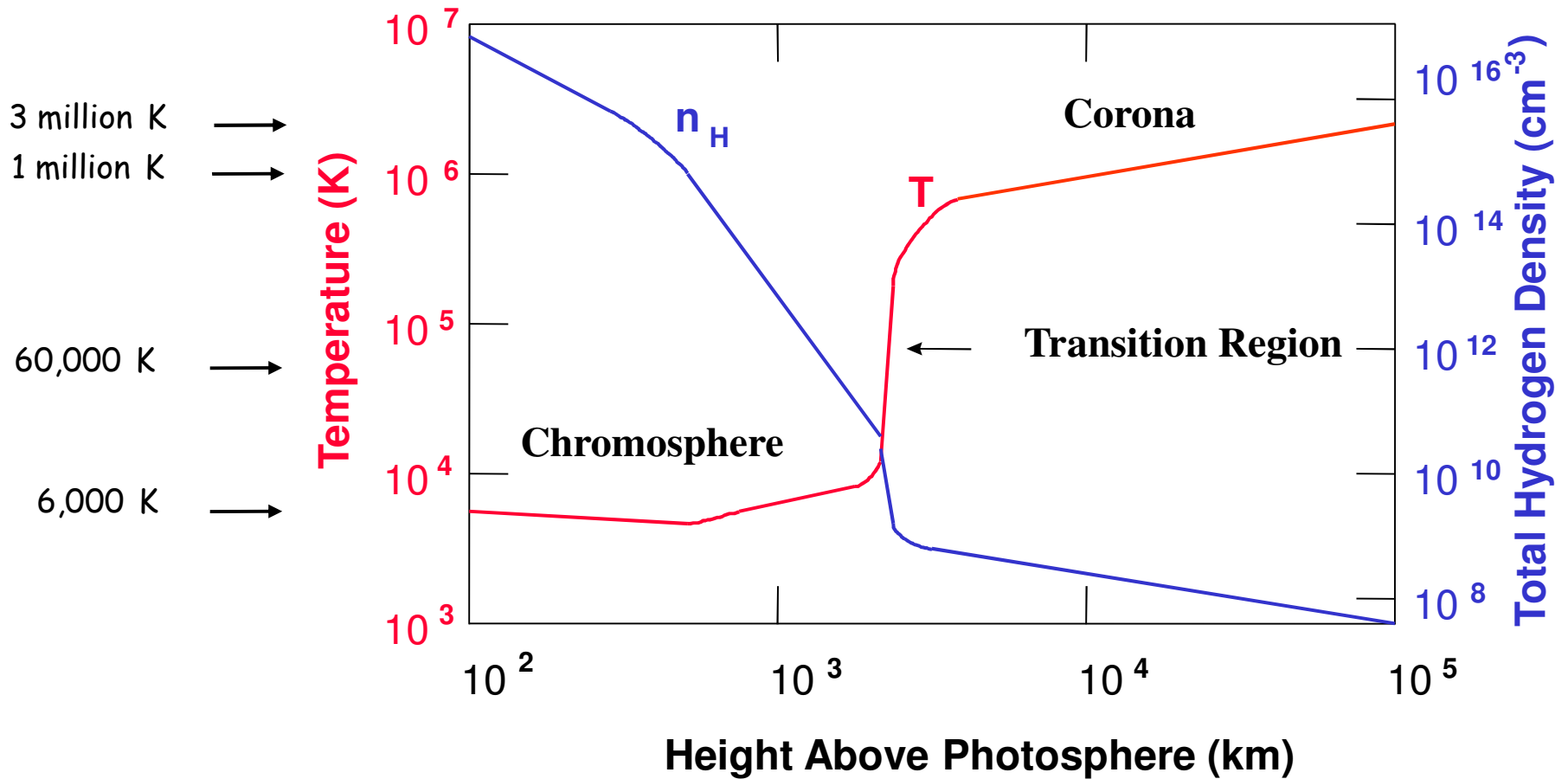
$$[\text{Fe}/\text{H}] = \log_{10} \left(\frac{N_{\text{Fe}}}{N_{\text{H}}} \right)_{\text{star}} - \log_{10} \left(\frac{N_{\text{Fe}}}{N_{\text{H}}} \right)_{\text{sun}}$$

measured in dex (e.g. if [Fe/H]=-1 the number density is 10 times smaller than on the Sun).

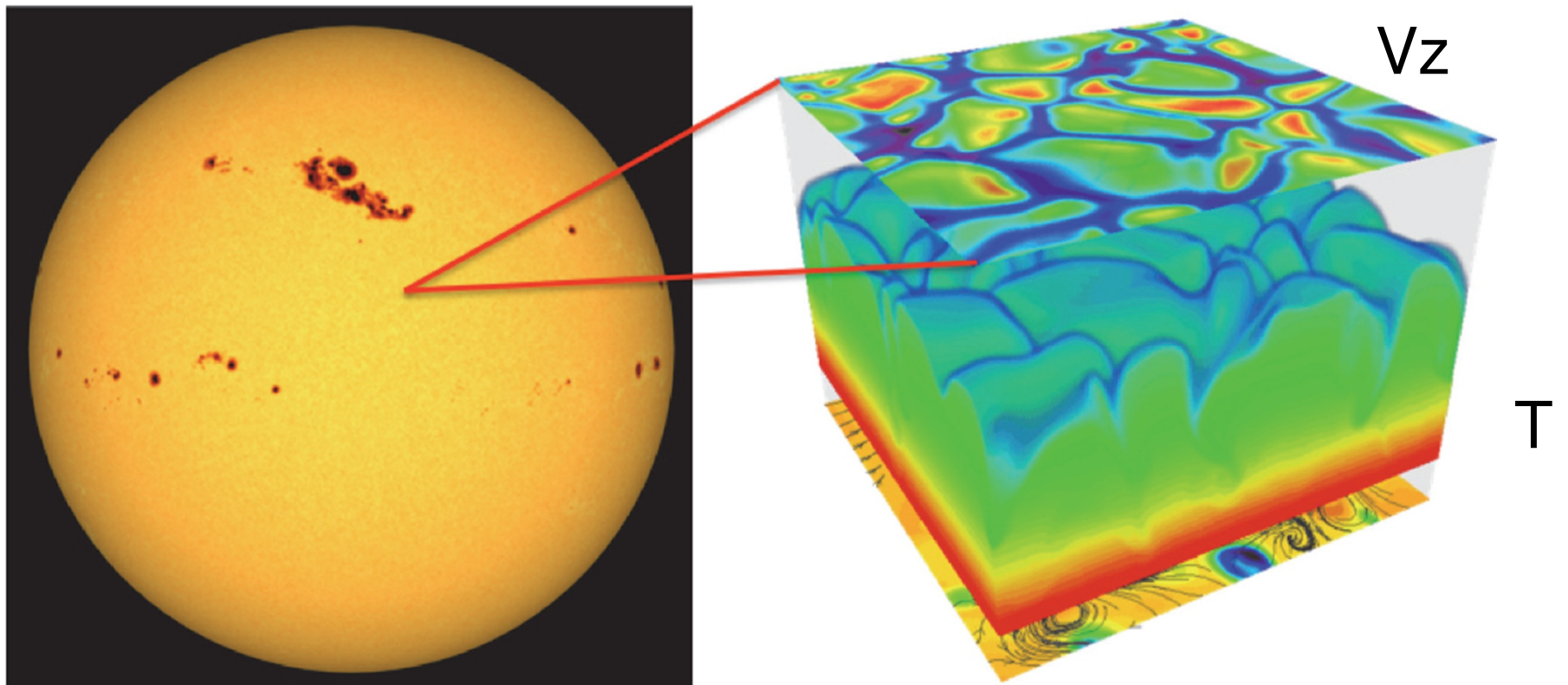
Determination of solar (stellar) abundances



Temperature & Density Structure of the Solar Atmosphere

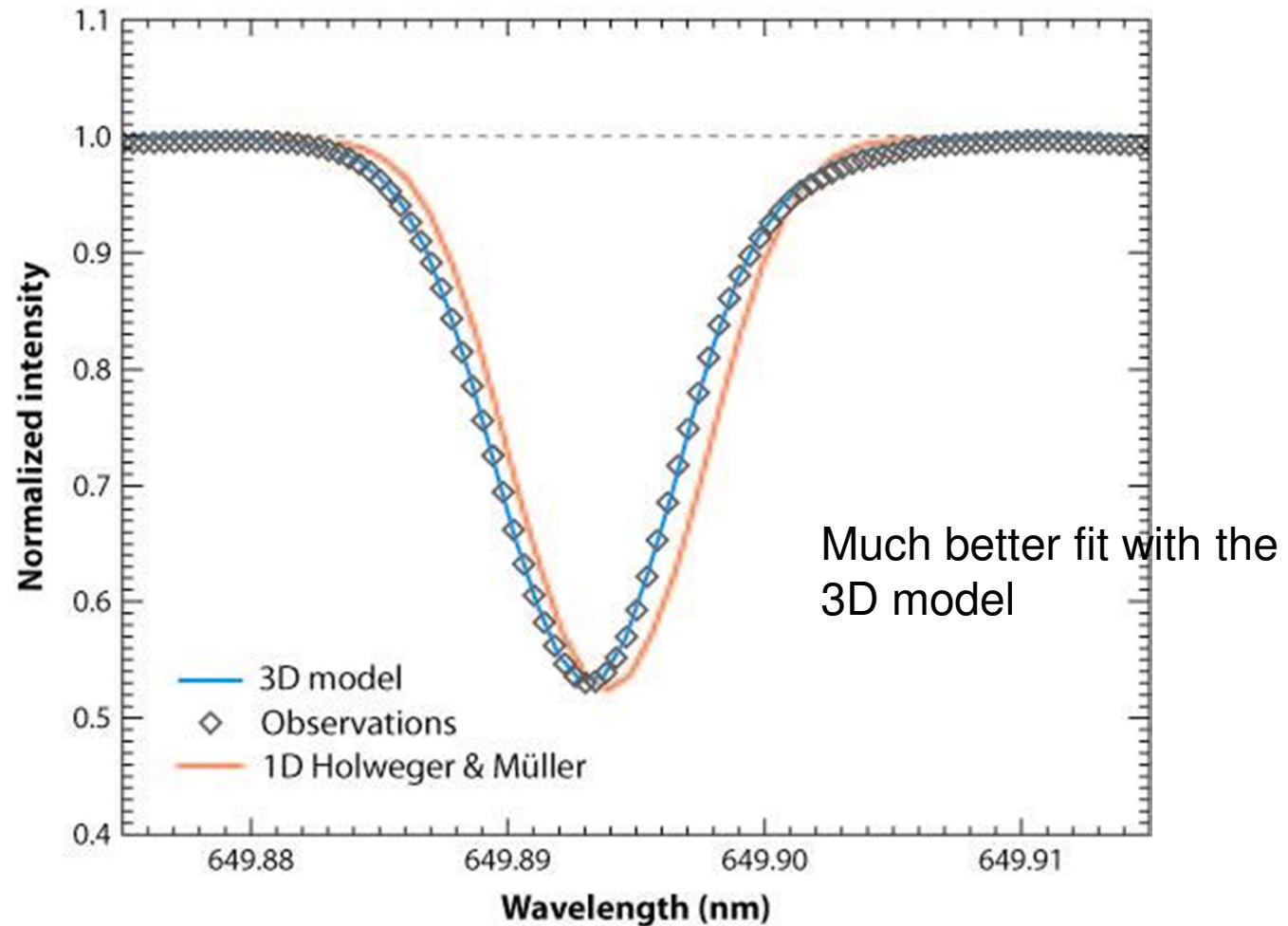


3D realistic simulation of the solar surface take into account all essential physics: stratification, gravity, radiative energy transfer, ionization, detailed chemical composition



Only small surface areas can be simulated on modern supercomputers

Example of fitting synthetic spectral line of Fe I from 1D and 3D models to observations




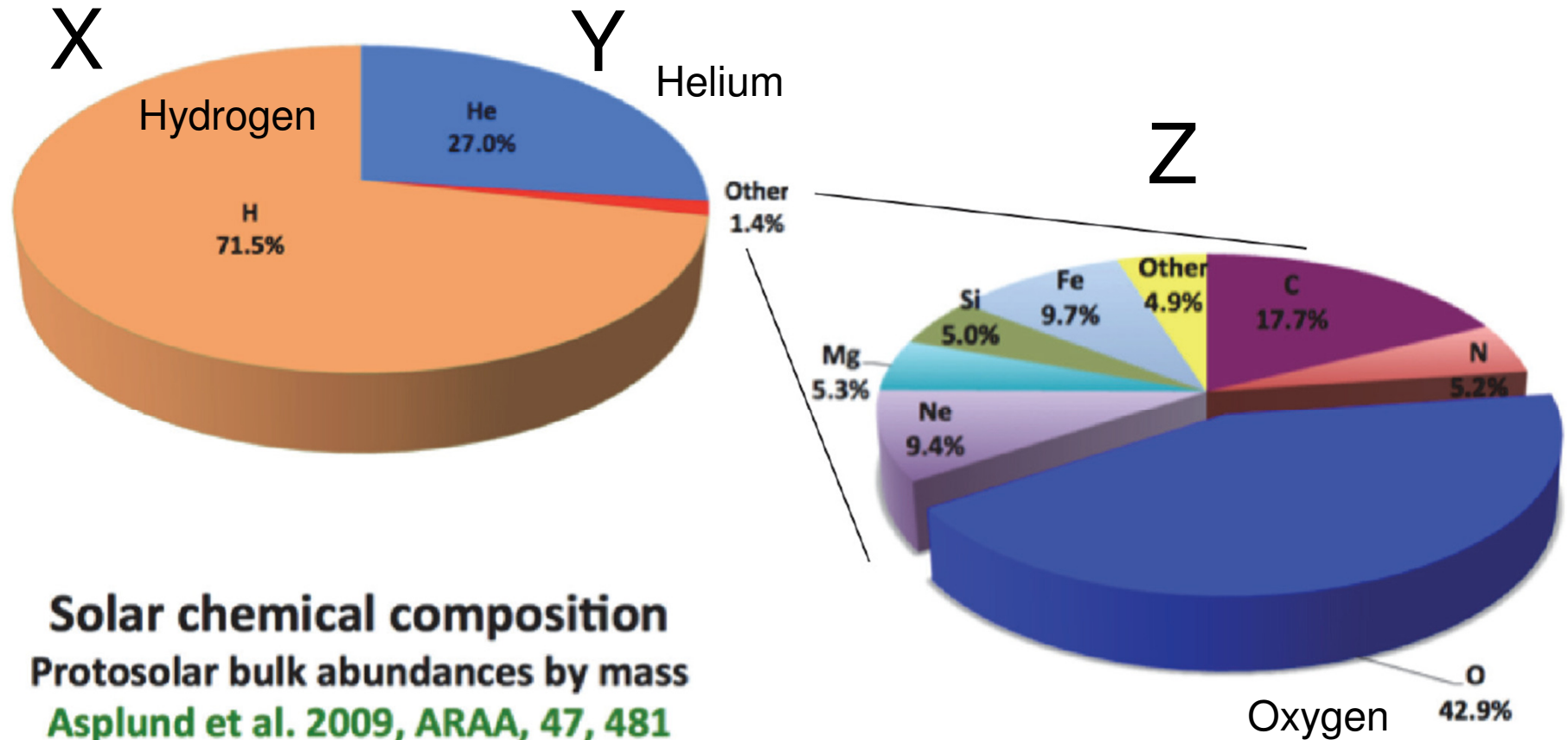
 Asplund M, et al. 2009.
Annu. Rev. Astron. Astrophys. 47:481–522

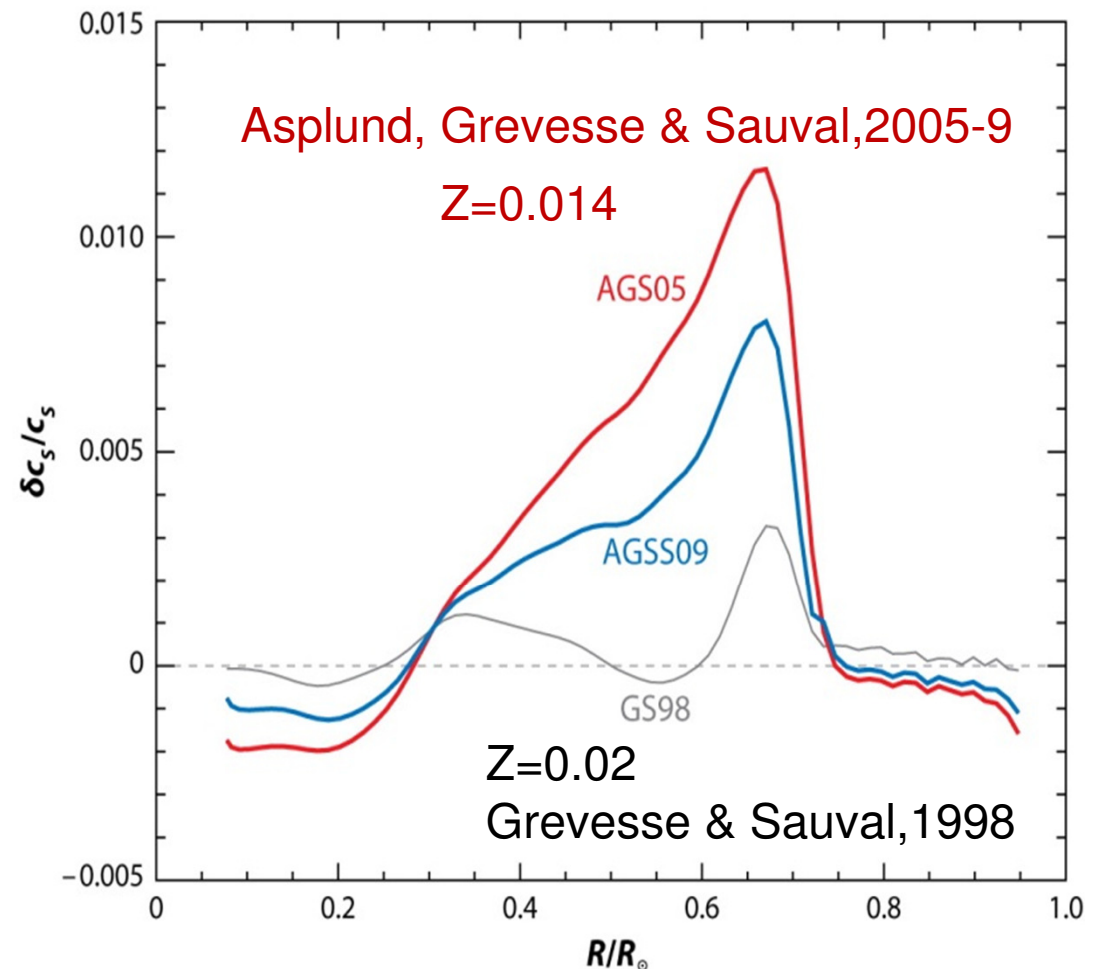
Illustration of the solar abundances (mass fractions)



The result of the 3D models was a substantially lower abundance of the heavy elements: $Z=0.014$ instead of 0.02 found using 1D models.

The low Z led to a “crisis” in helioseismology and solar modeling

- For a given chemical composition, X, Y, Z, the structure of the Sun is calculated using the Standard Stellar Evolution Theory.
- The distribution of the sound speed as a function of radius is determined by helioseismology, and can be compared with the solar model.
- For $Z=0.02$ the solar model is in excellent agreement with helioseismology.
- However, for $Z=0.014$ the disagreement is very large. The source of discrepancy is still unknown.



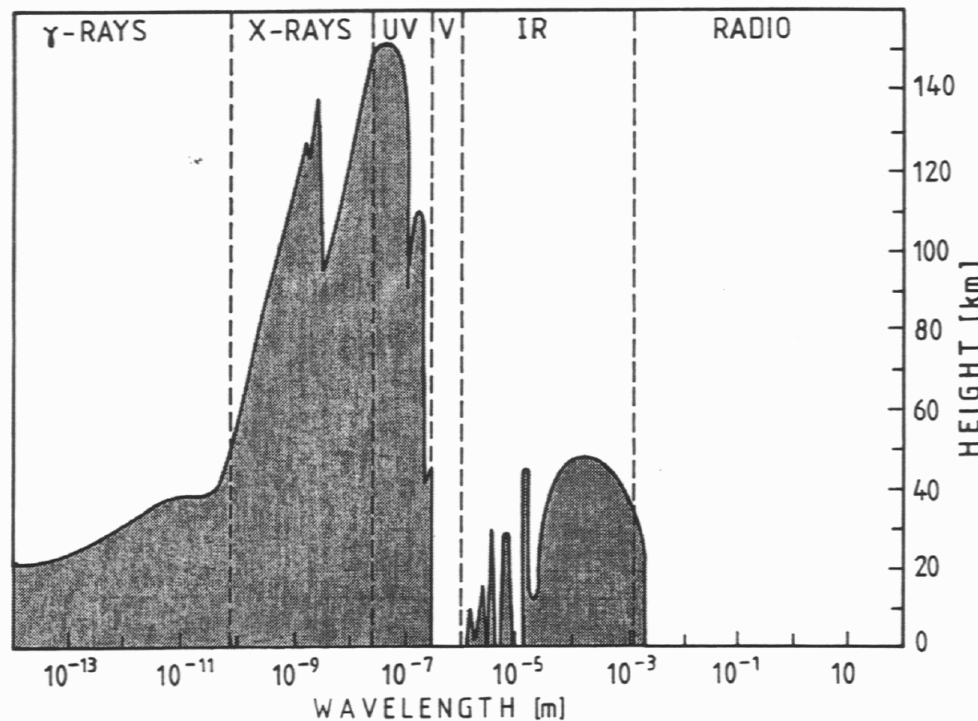
Luminosity

The solar luminosity, L_{\odot} , is the the total output of electromagnetic energy per unit time. It is measured from space because the Earth's atmosphere attenuates the solar radiation.

$$L_{\odot} = (3.828 \pm 0.006) \times 10^{33} \text{ erg / s.}$$

The total irradiance at 1 AU ("solar constant"):

$$S = L_{\odot} / 4\pi A^2 \approx 1367 \pm 2 \text{ W/m}^2 .$$



Absorption in the Earth's atmosphere.

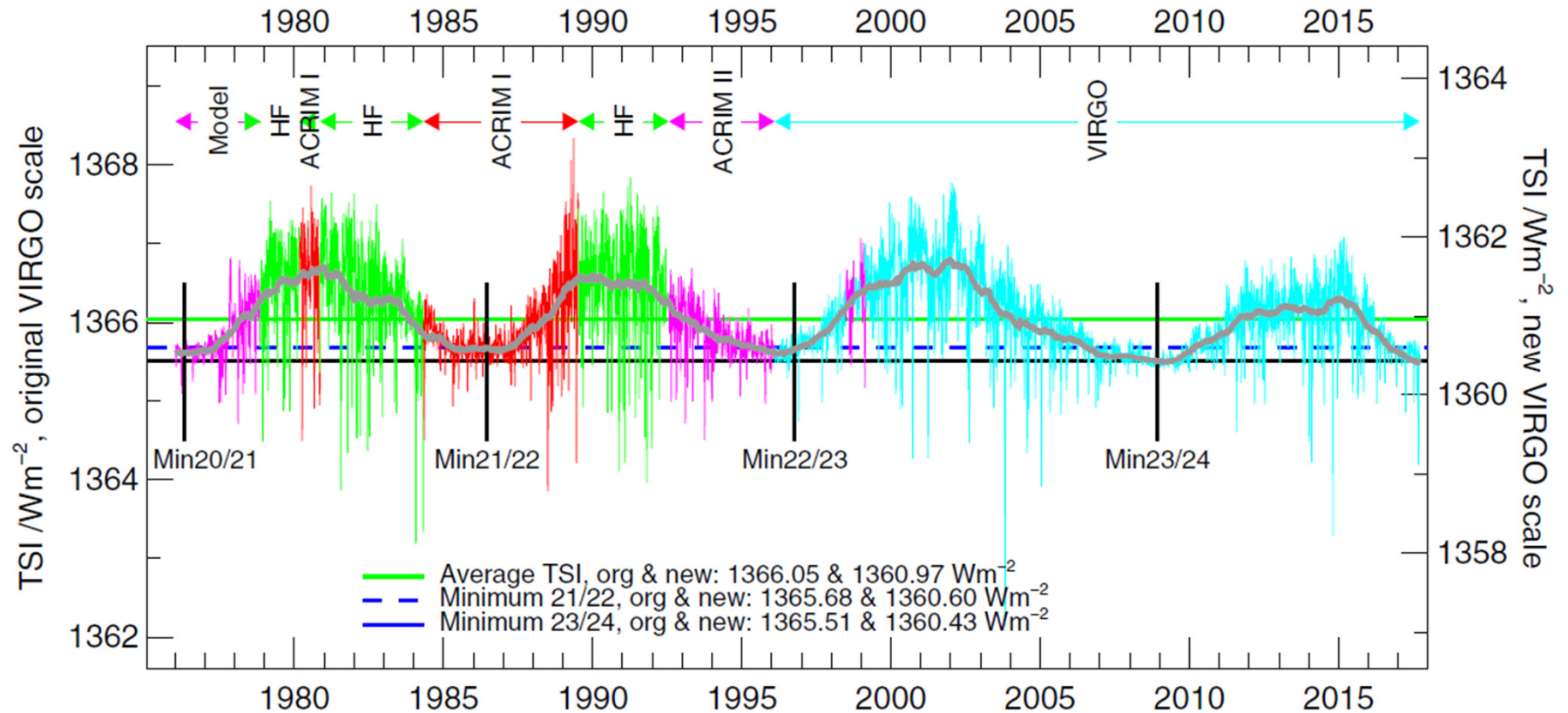
The edge of the shaded area marks the height where the radiation is reduced to 1/2 of its original strength.

UV - ultraviolet; V- visible; IR - infrared.

Irradiance variations

The total irradiance at 1 AU ("solar constant"):

$$S = L_{\odot} / 4\pi A^2 \approx 1367 \pm 2 \text{ W/m}^2.$$



The composite total irradiance from 1977 to 2018.

Note the variation with the solar activity cycle of order 0.1%

Faint young Sun paradox

- The Standard Stellar Evolution theory shows that the Sun's luminosity increased by 28% over the Sun's life of 4.6 billion years.
- If the solar energy output was 28% lower then oceans would freeze. But geological records show that this was not the case, and the surface was warm.
- Possible solutions:
 - Earth's atmosphere had more greenhouse gases
 - Earth produced more internal heat
 - The Sun was more massive, and lost mass because of strong solar wind – this is a hot topic of current research in astronomy (“The Sun in Time” project).

Effective temperature of the Sun

The effective temperature is determined by:

$$L_{\odot} = 4\pi R_{\odot}^2 \sigma T_{\text{eff}}^4,$$

where $\sigma = 5.67032 \times 10^{-11}$ erg/cm² K⁴ is the Stefan-Boltzmann constant.

$$T_{\text{eff}} = 5772 \pm 2.5 \text{ K}$$

Spectral energy distribution

The energy flux, $F(\lambda)$, is the emitted energy per unit area, time and wavelength interval.

The spectral irradiance:

$$S(\lambda) = F(\lambda)R_{\odot}^2/(1 \text{ AU})^2.$$

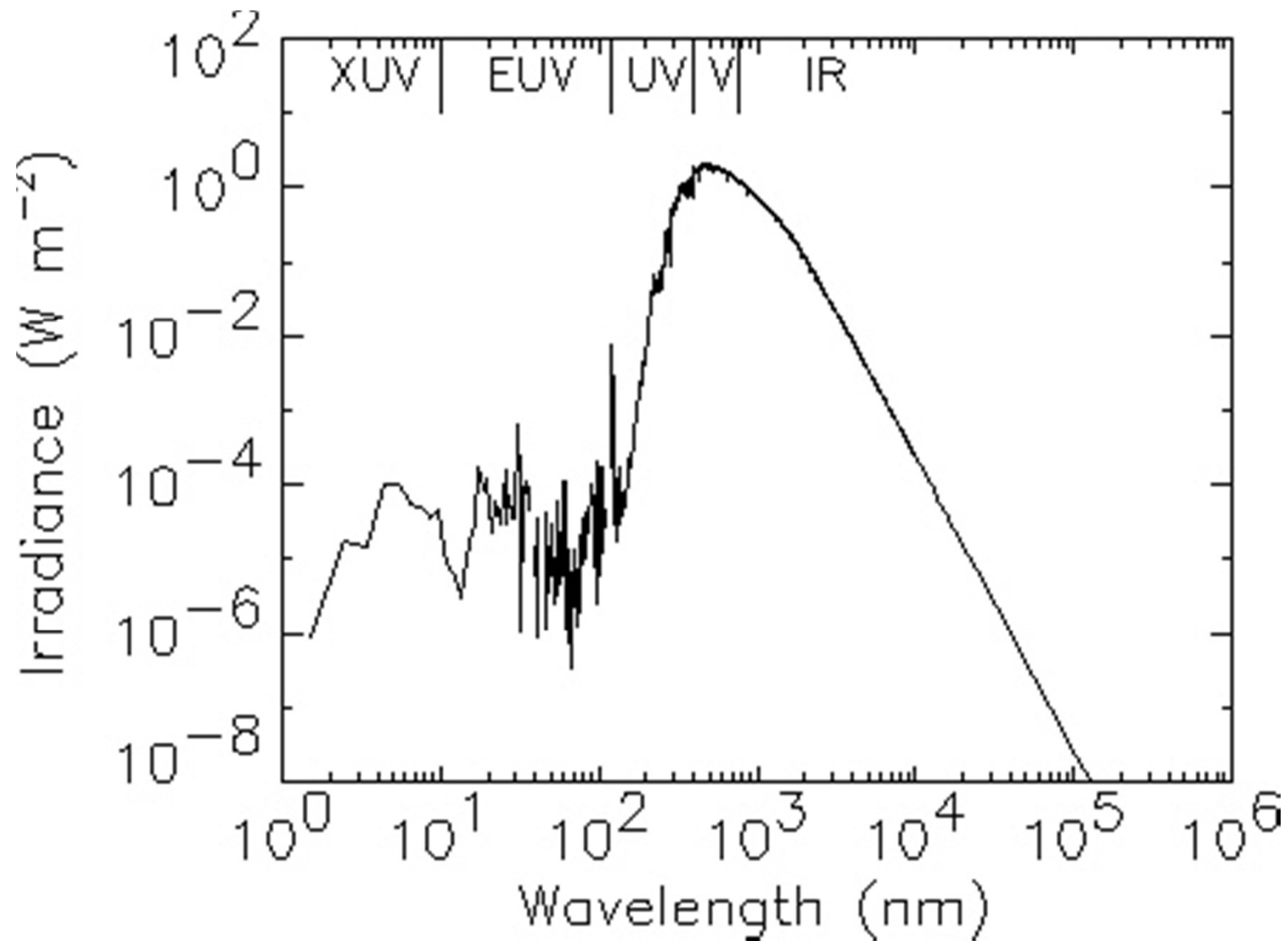
Intensity, $I(\theta, \lambda)$, is the energy emitted per unit area, time, wavelength interval, and sterad. It depends on angular distance θ from the normal to the surface.

$$F(\lambda) = 2\pi \int_0^{\pi} I(\theta, \lambda) \cos \theta \sin \theta d\theta.$$

(check this).

The limb-darkening function is $I(\theta, \lambda)/I(0, \lambda)$

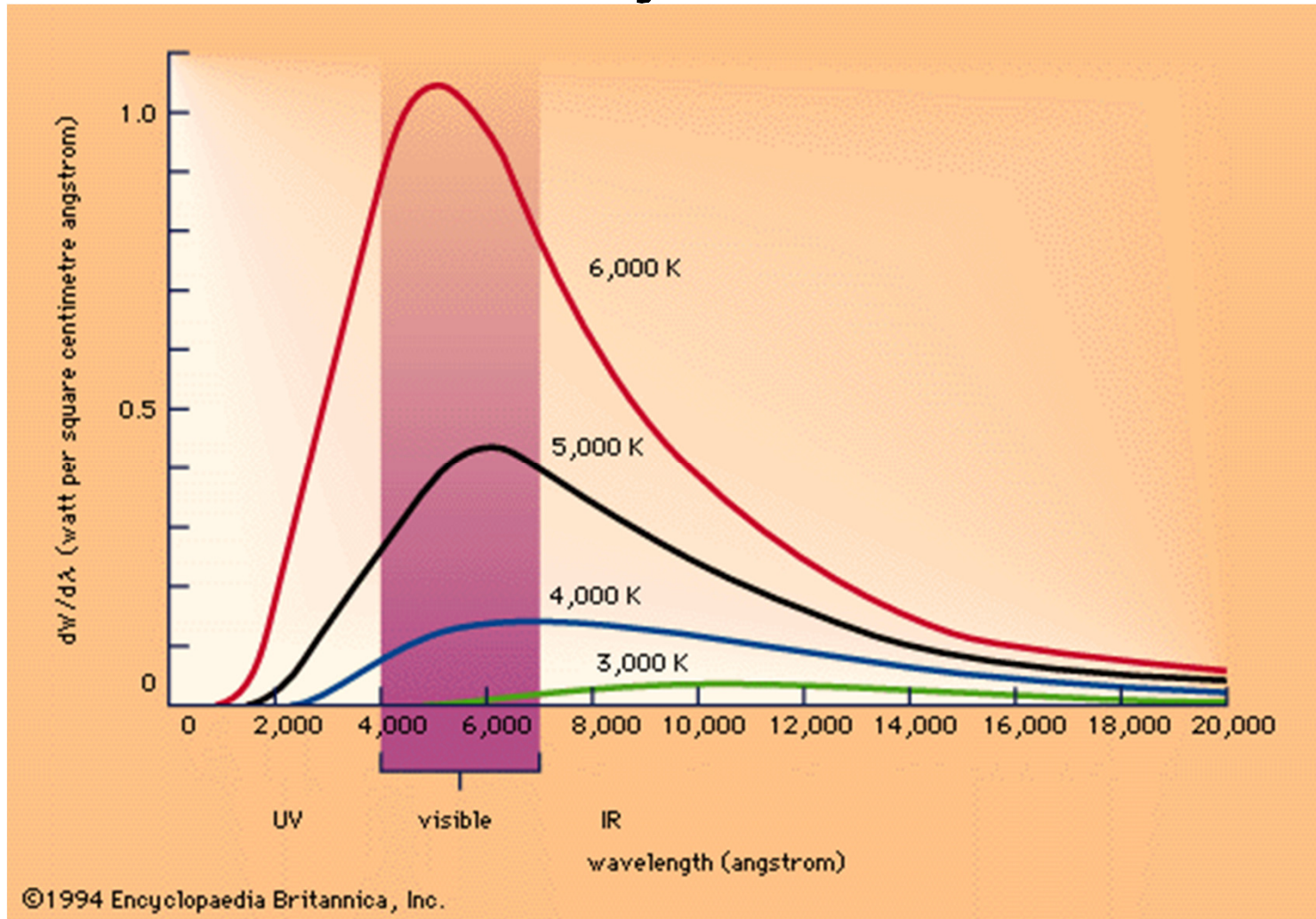
Solar irradiance spectrum



1 Angstrom = 10⁻¹⁰ m = 10⁻⁸ cm = 0.1 nm

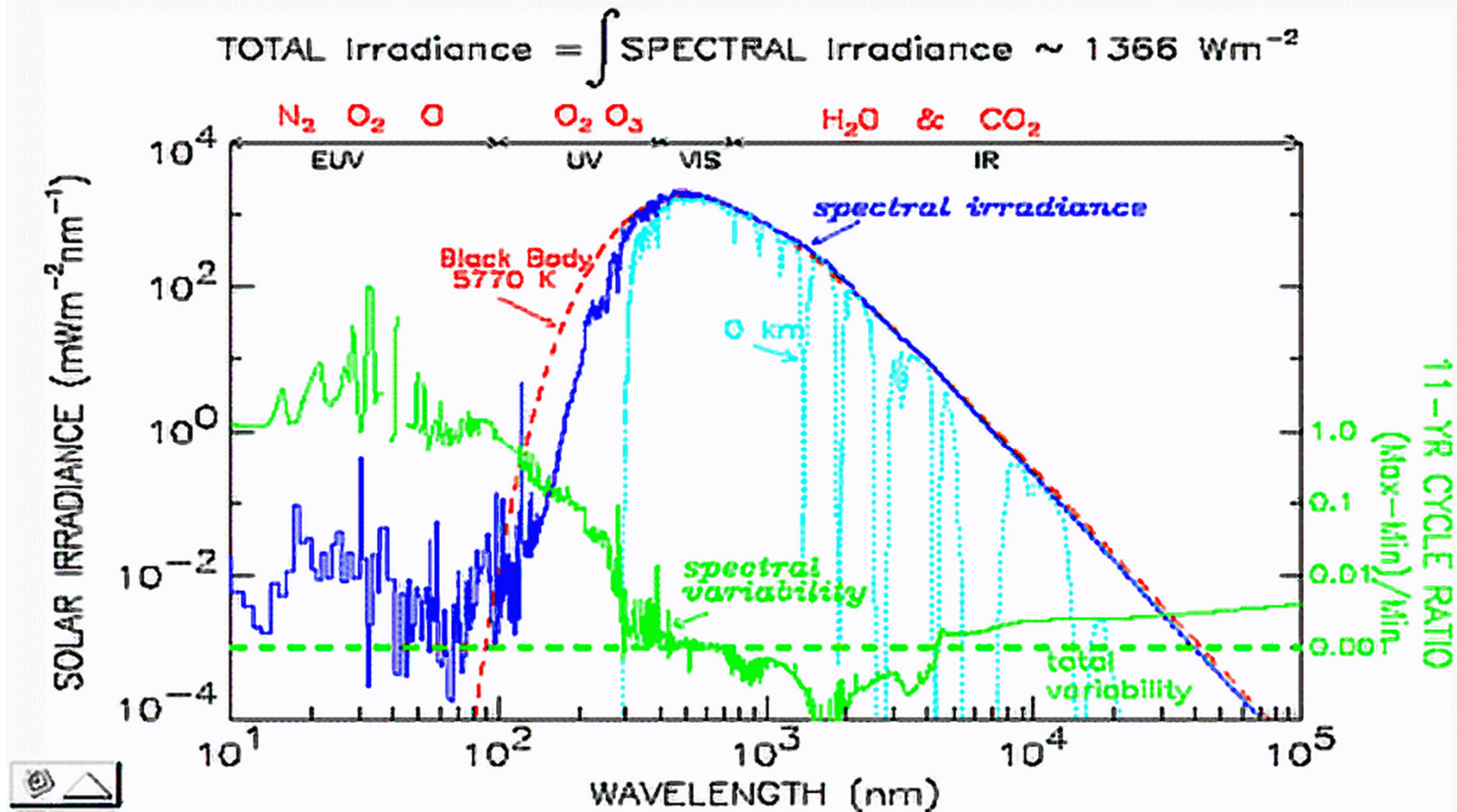
1 nm = 10 Å

Black body radiation



Black body spectrum depends only on temperature

SOLAR SPECTRUM, VARIABILITY and ATMOSPHERIC ABSORPTION



Spectral energy distribution

The energy flux, $F(\lambda)$, is the emitted energy per unit area, time and wavelength interval.

The spectral irradiance:

$$S(\lambda) = F(\lambda)R_{\odot}^2/(1 \text{ AU})^2.$$

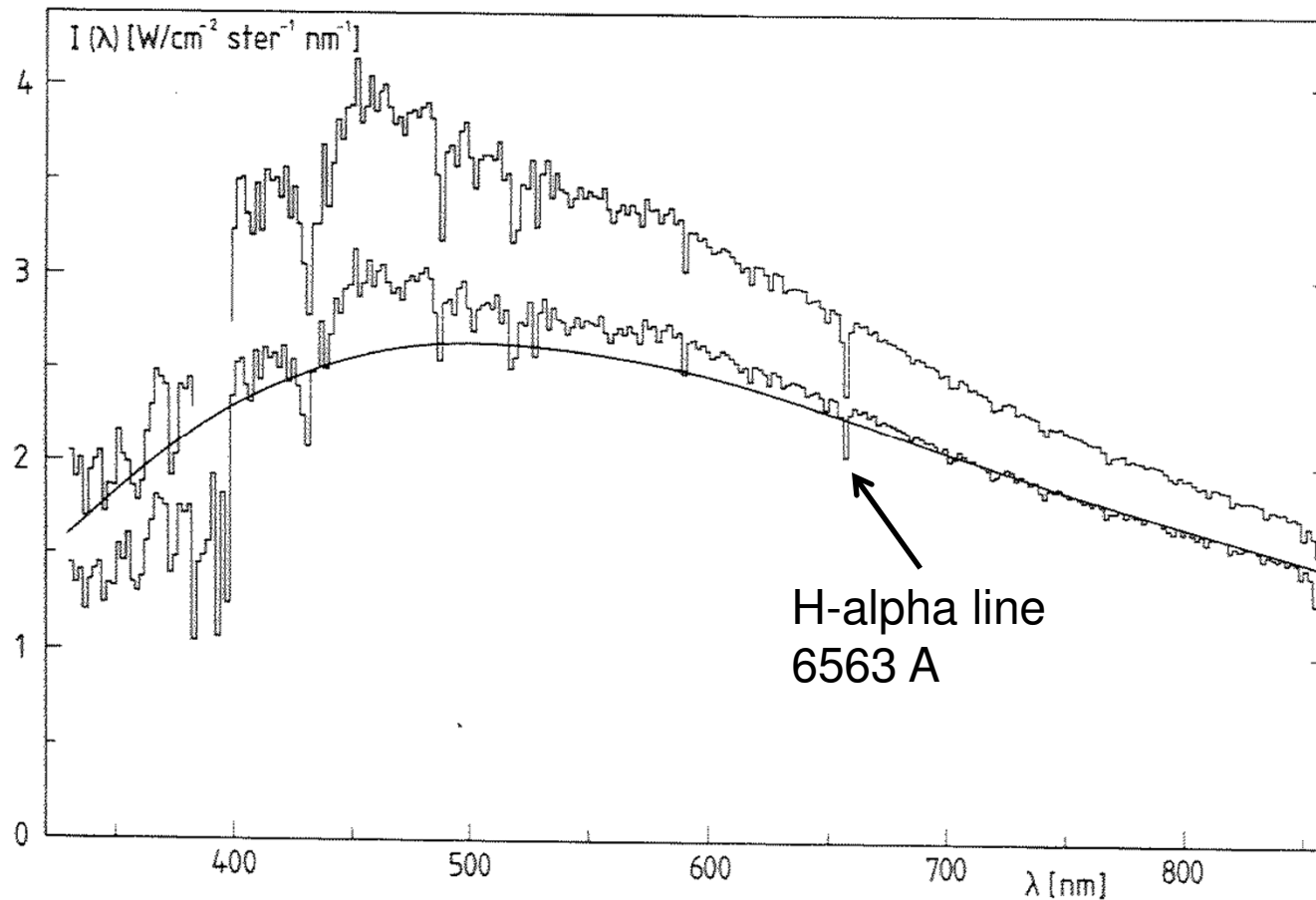
Intensity, $I(\theta, \lambda)$, is the energy emitted per unit area, time, wavelength interval, and sterad. It depends on angular distance θ from the normal to the surface.

$$F(\lambda) = 2\pi \int_0^{\pi} I(\theta, \lambda) \cos \theta \sin \theta d\theta.$$

(check this).

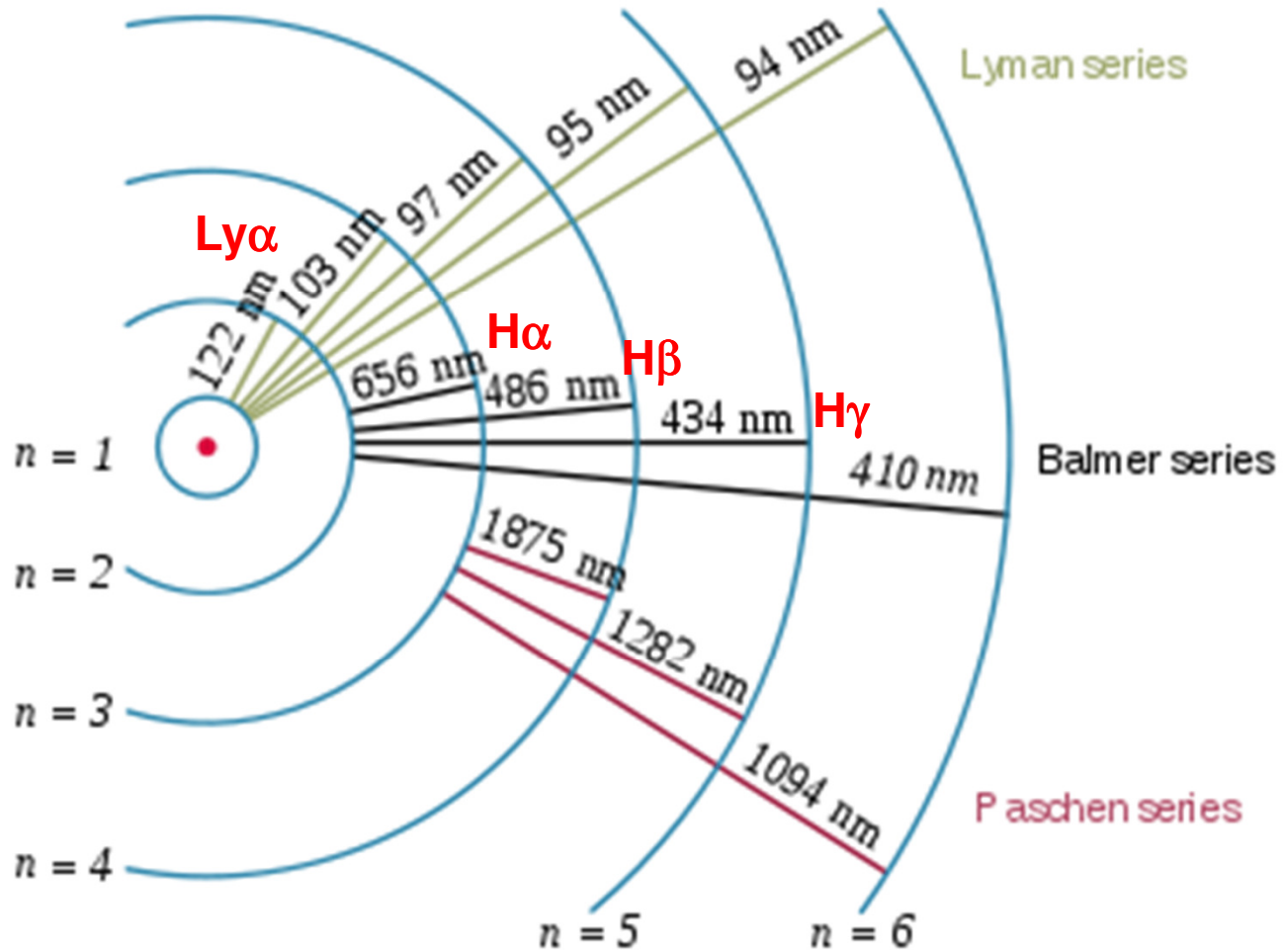
The limb-darkening function is $I(\theta, \lambda)/I(0, \lambda)$

Visible spectrum

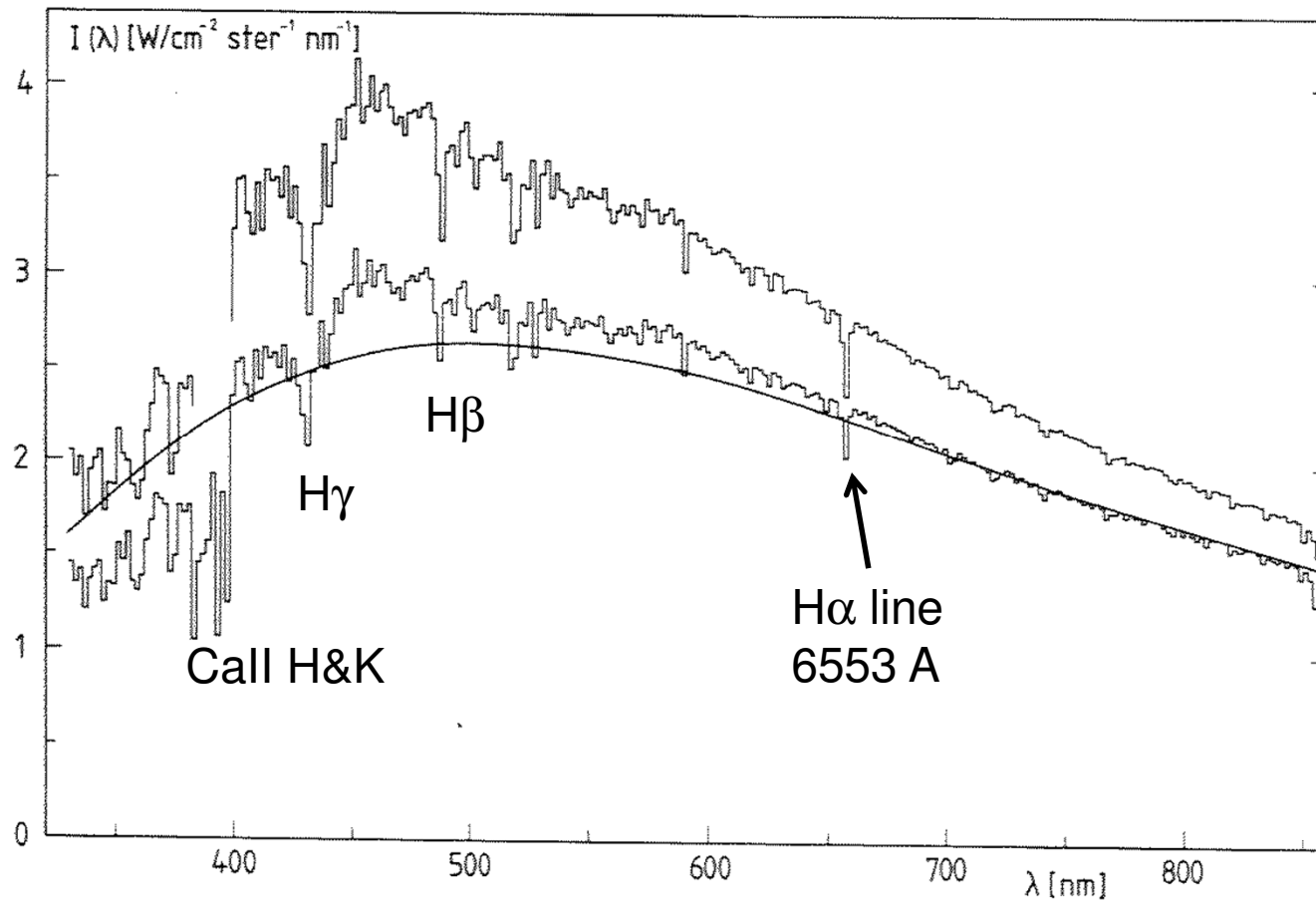


The visible spectrum. The upper curve - $I(0, \lambda)$; the lower curve - $F(\lambda)/\pi$ (intensity averaged over the disk); The smooth curve is a black-body spectrum at $T = T_{\text{eff}} = 5557 \text{ K}$. Note the hydrogen H_{α} absorption line at $\lambda = 656.3 \text{ nm}$.

Hydrogen series

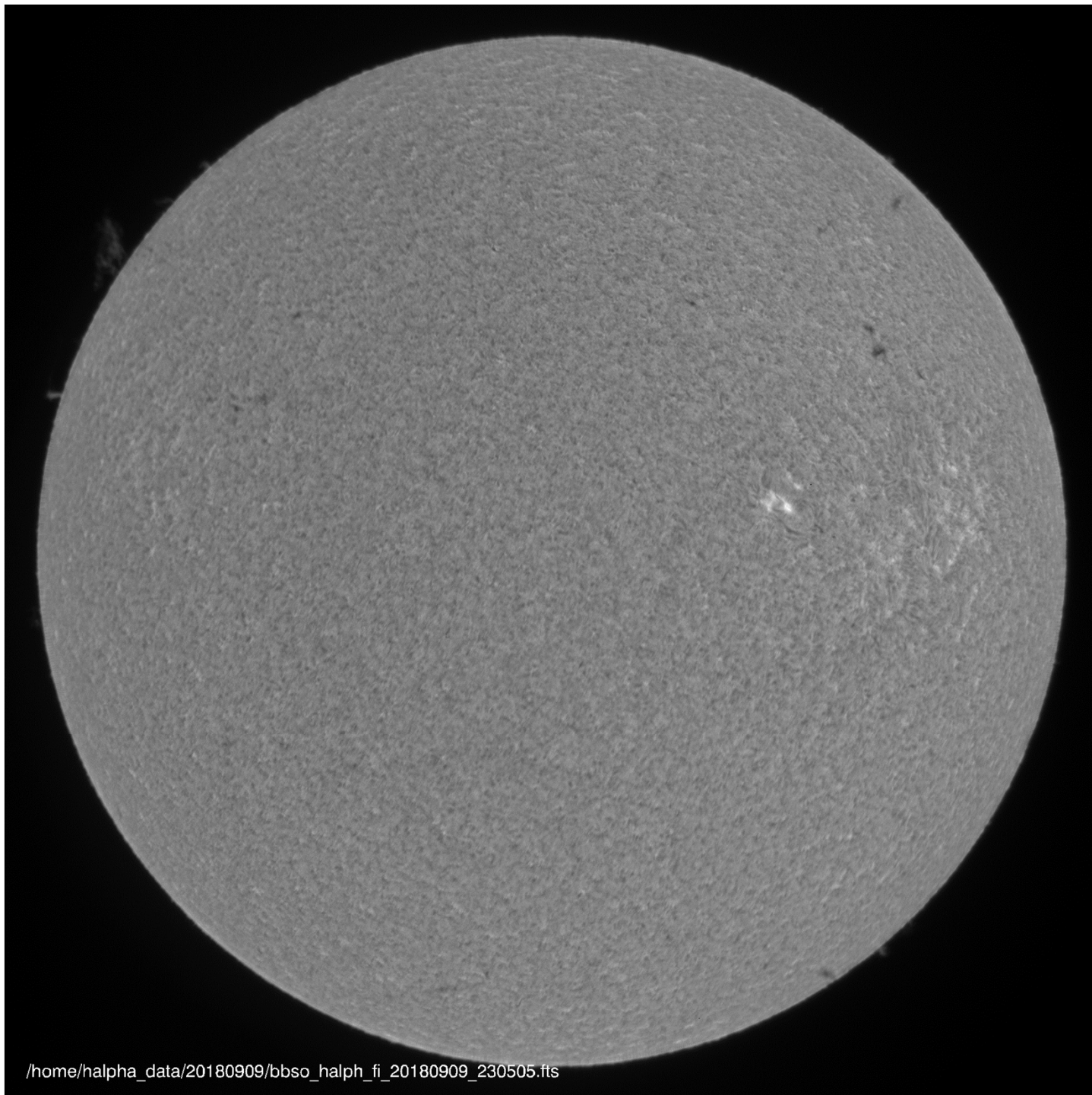


Visible spectrum



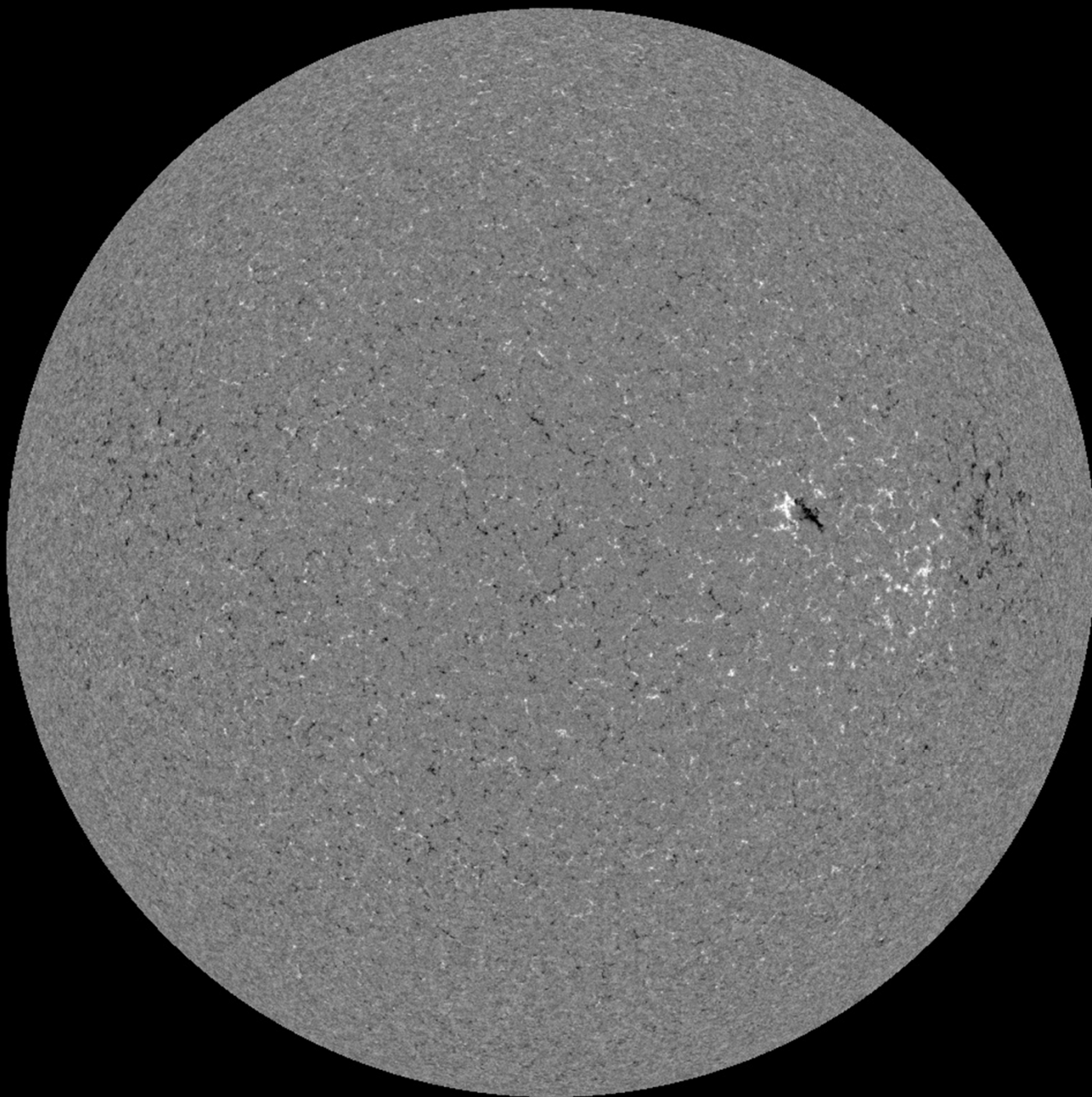
The visible spectrum. The upper curve - $I(0, \lambda)$; the lower curve - $F(\lambda)/\pi$ (intensity averaged over the disk); The smooth curve is a black-body spectrum at $T = T_{\text{eff}} = 5557 \text{ K}$. Note the hydrogen H_{α} absorption line at $\lambda = 656.3 \text{ nm}$.

H α image from
BBSO
September 9,
2018



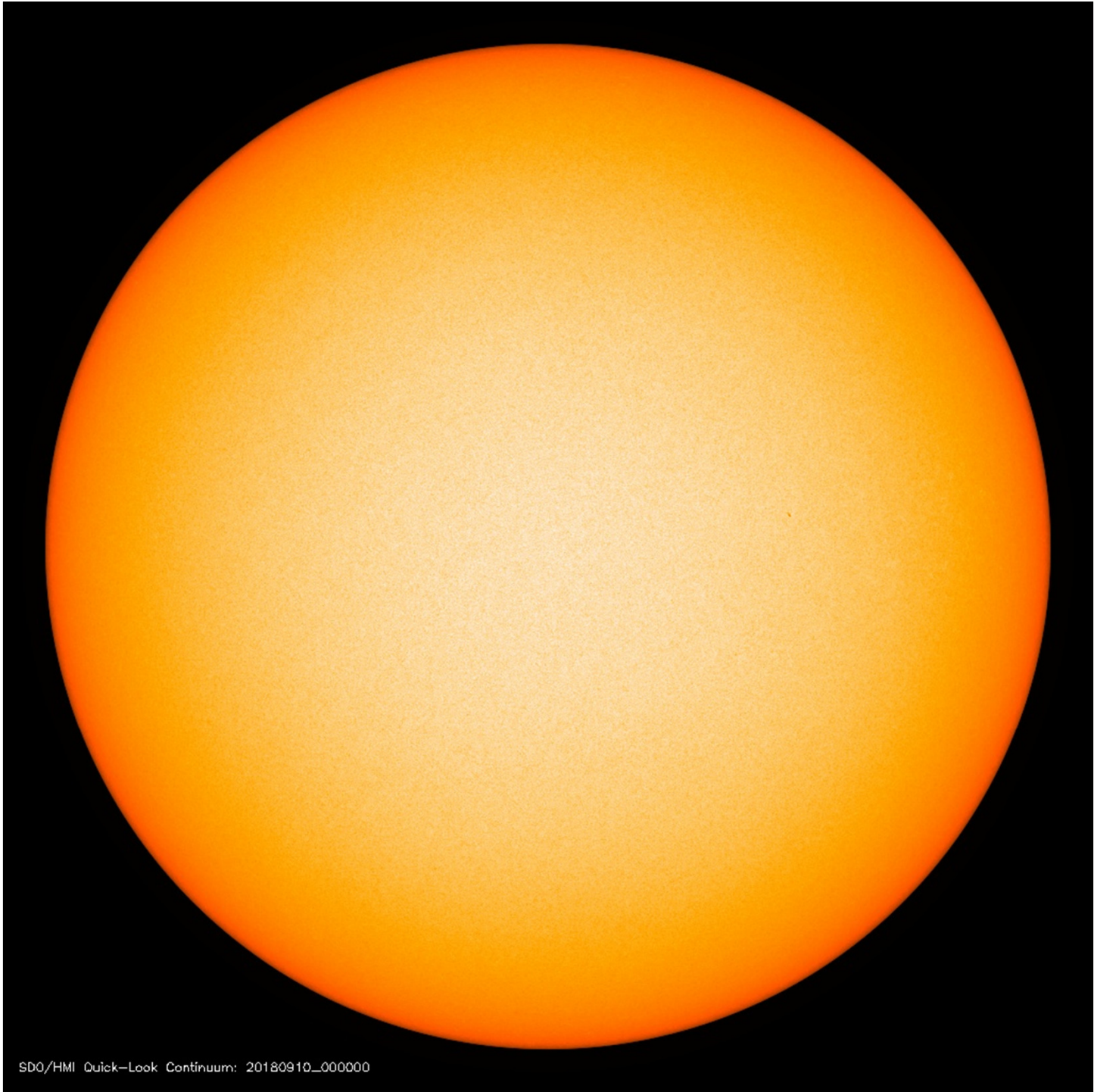
/home/halpha_data/20180909/bbso_halph_fi_20180909_230505.fits

Magneto-
gram
SDO/HMI



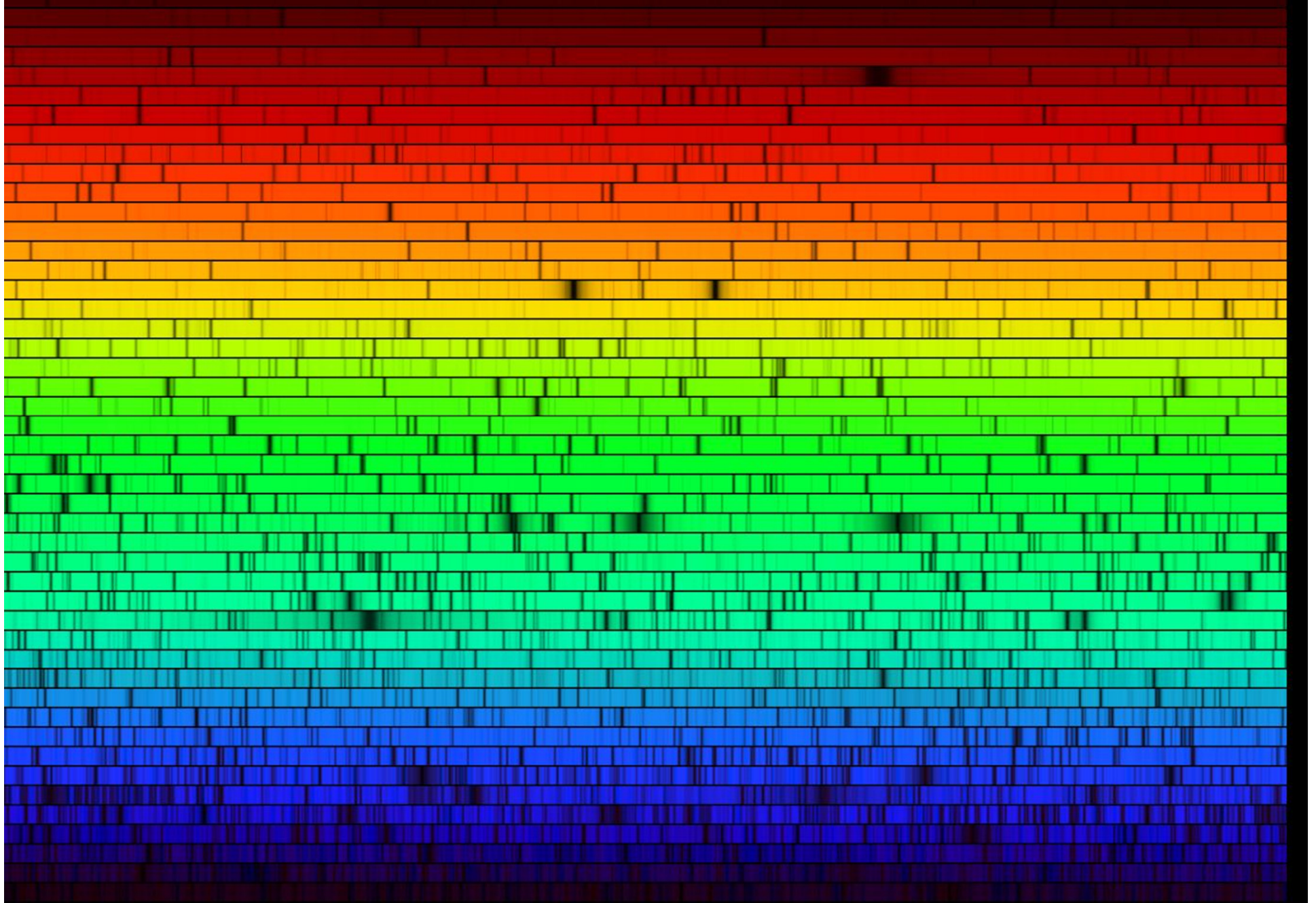
SDO/HMI Quick-Look Magnetogram: 20180910_000000

Continuum
Image
SDO/HMI

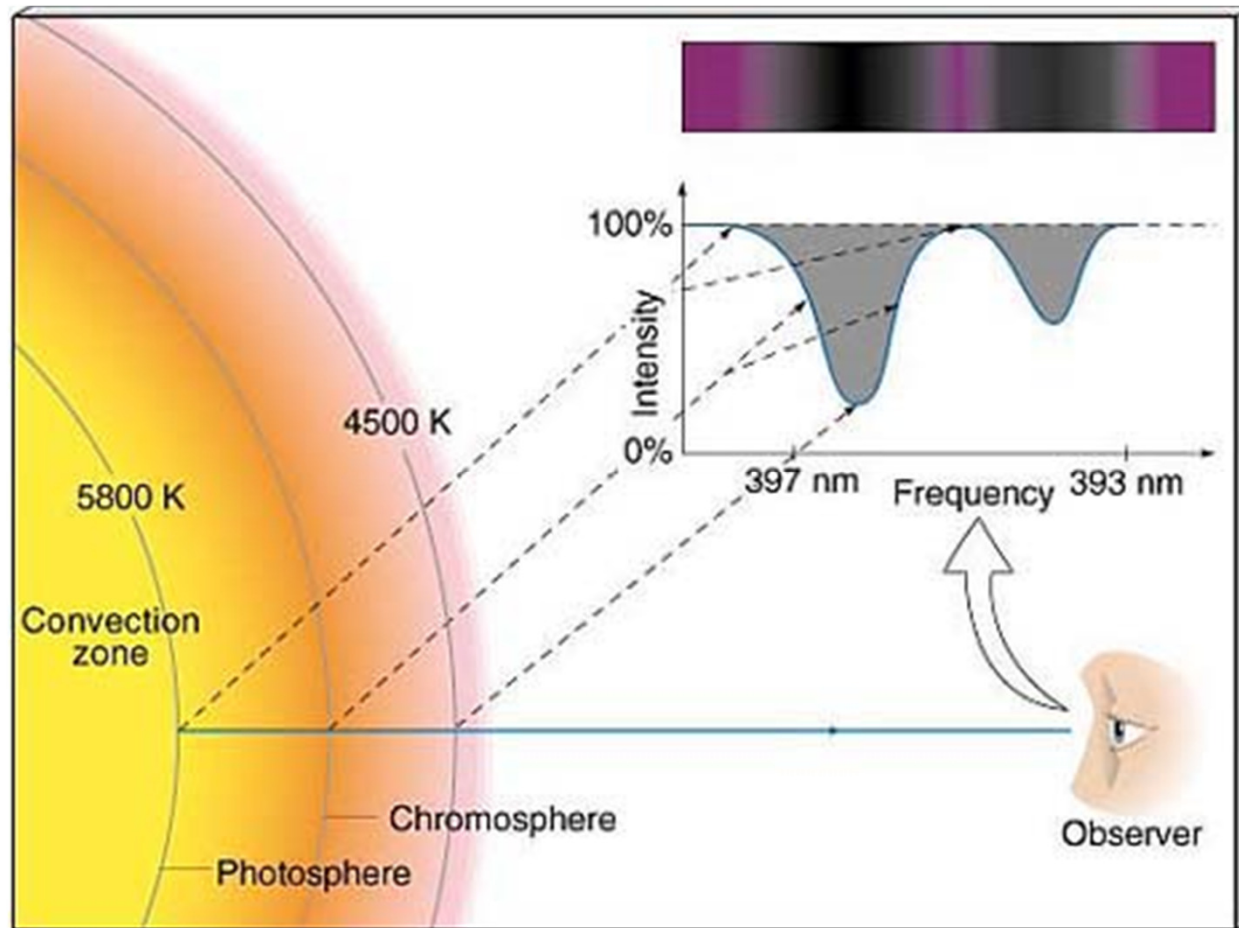


SDO/HMI Quick-Look Continuum: 20180910_000000

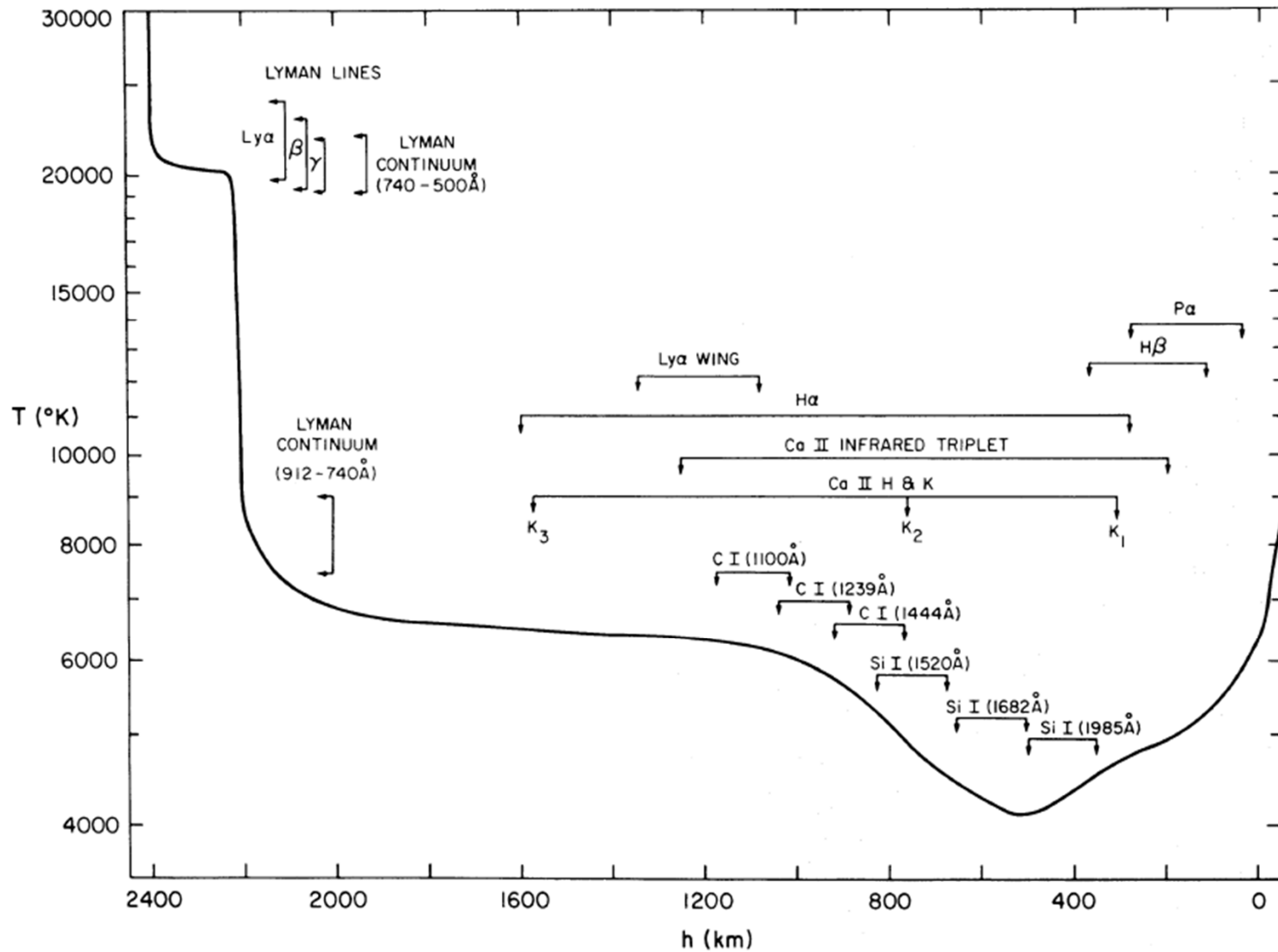
Visible solar spectrum with absorption (Fraunhofer) lines



Different parts of Fraunhofer lines are formed in different layers: the line core is formed higher than the line wings



VAL (Vernazza, Avrett, Loeser) model of the solar atmosphere



Color indices

Color indices are rough characteristics of the spectral energy distribution.

$$U - B = -2.5 \left(\log \int_0^\infty S(\lambda) E_U(\lambda) d\lambda - \log \int_0^\infty S(\lambda) E_B(\lambda) d\lambda \right) + C_{UB}$$

$$B - V = -2.5 \left(\log \int_0^\infty S(\lambda) E_B(\lambda) d\lambda - \log \int_0^\infty S(\lambda) E_V(\lambda) d\lambda \right) + C_{BV}$$

where E_U, E_V, E_B are ultraviolet, blue and visible filter functions about 100 nm wide, centered at 365, 440, and 548 nm respectively. Constants C_{UB} and C_{BV} are chosen that both $U - B$ and $B - V$ are zero for A0-type stars.

The Sun has $U - B = 0.20$ and $B - V = 0.66$.

Infrared spectrum

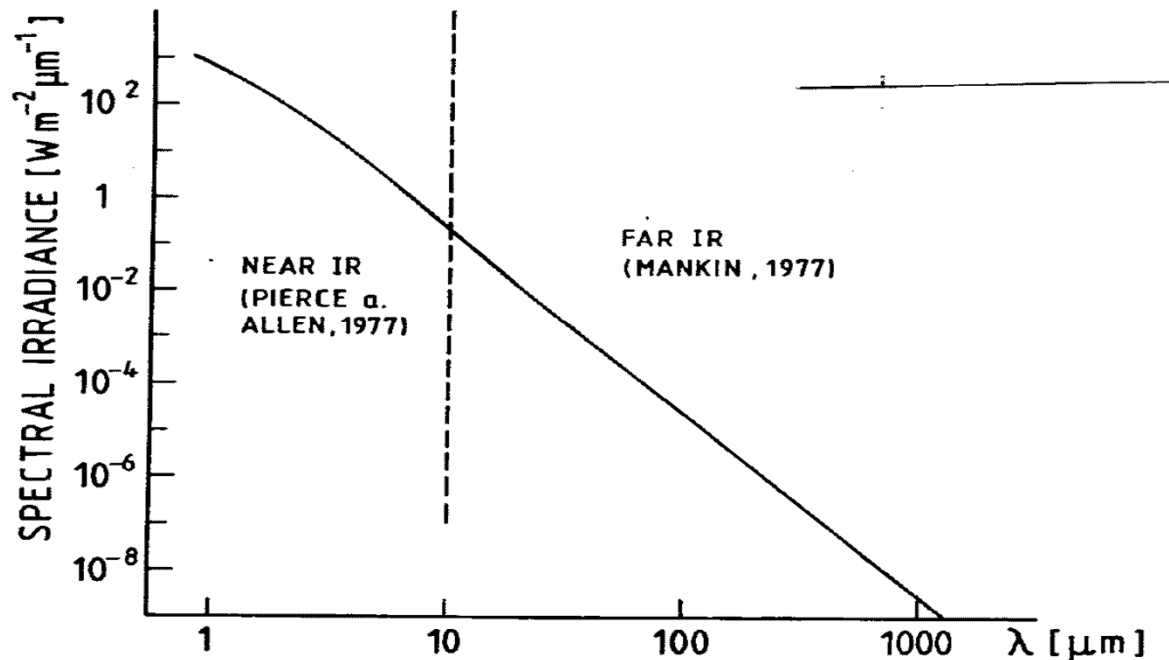
About 44% of the energy is emitted above $0.8 \mu\text{m}$. The spectrum is approximated by the

Reileigh-Jeans relation: $S(\lambda) \approx 2\pi ckT \lambda^{-4} (R_{\odot} / 1 \text{ AU})^2$.

The brightness temperature, T_B , is defined by $I_{\lambda} = B_{\lambda}(T_B)$, where I_{λ} is the observed absolute intensity, $B(T)$ is the Kirchhoff-Plank function:

$$B_{\nu}(T) = \frac{2h\nu^3}{c^2} \frac{1}{\exp(h\nu / kT) - 1} \text{ per unit frequency, or}$$

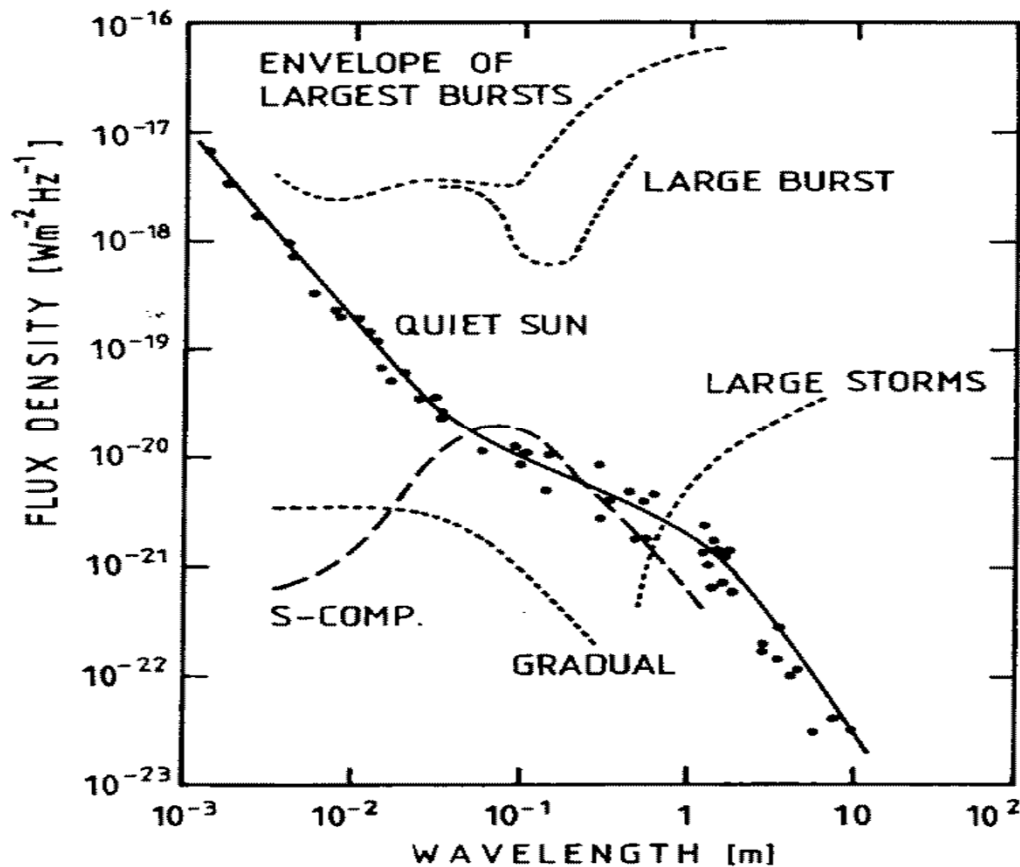
$$B_{\lambda}(T) = \frac{2hc^2}{\lambda^5} \frac{1}{\exp(hc / \lambda kT) - 1} \text{ per unit wavelength; } T_B \approx 5000 \text{ K at } \lambda = 10 \mu\text{m}.$$



The infrared spectral irradiance.

Radio spectrum

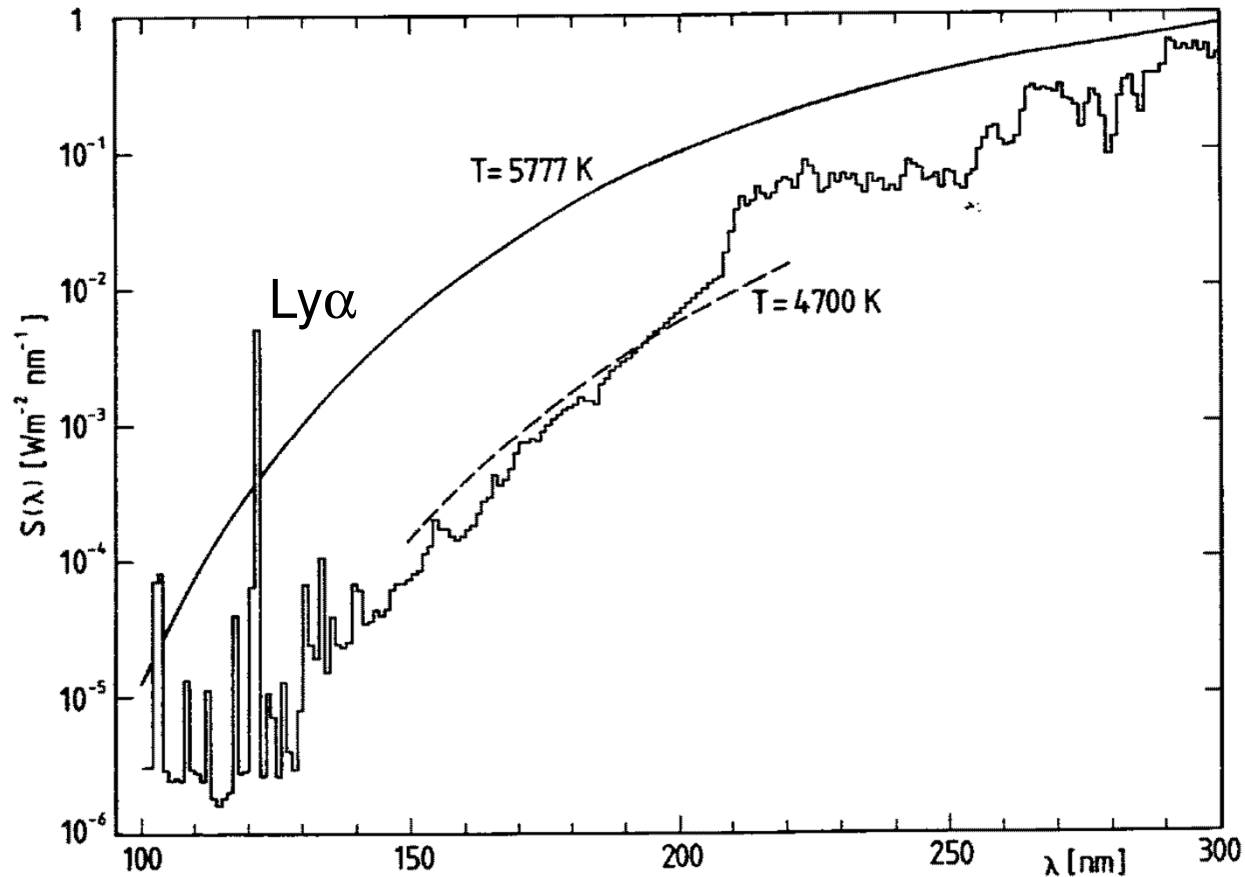
The radio spectrum begins at $\lambda = 1$ mm. The energy is often given per unit frequency rather than per unit wavelength. For quiet Sun it continues smoothly from the infrared. Discovered in 1942.



Solar radio emission.

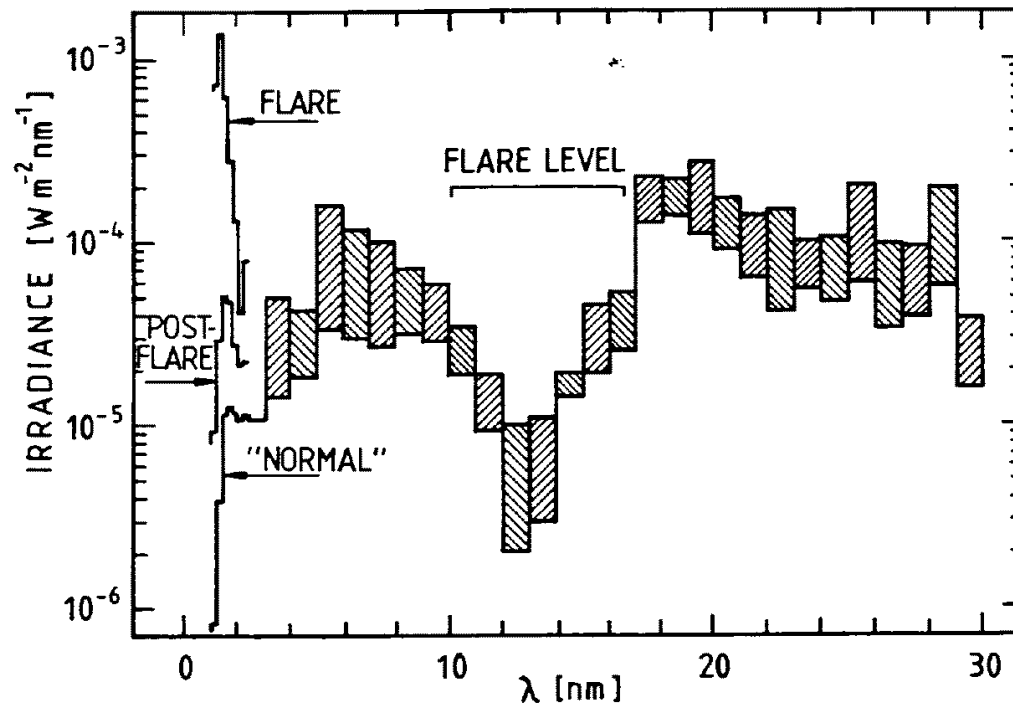
Dots and solid curve - quiet Sun; dashed - slowly varying component (*s-component*); dotted curves - rapid events (*bursts*). Note the transition between $\lambda = 1$ cm and $\lambda = 1$ m. There is a transition in T_B from 10^4 K to 10^6 K - transition from the solar chromosphere to corona.

UV spectrum



UV irradiance. The solid and dashed smooth curves are black-body spectra. Note the sharp decrease at $\lambda = 210 \text{ nm}$ due to the ionization of Al I. Absorption lines are mostly above 200 nm . Below 150 nm emission lines dominate the spectrum. The most prominent is the Lyman α line at 121.57 nm . The spectrum is highly variable.

EUV and X-ray spectrum



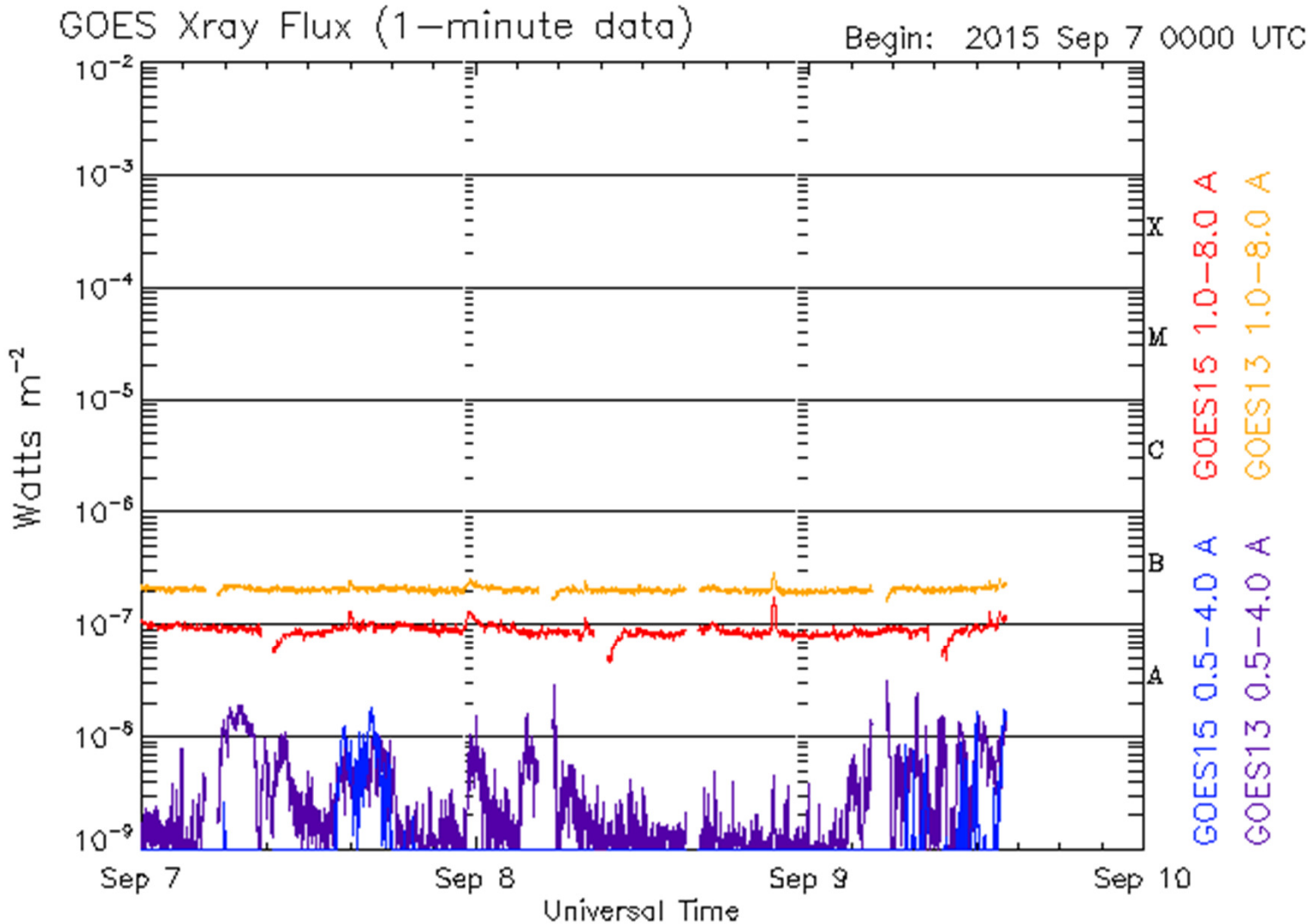
EUV is below 120 nm. It is highly variable, and characterized by a large number of emission lines from highly ionized atom, e.g. Fe XVI. The range of T_B is from 8000 K to 4×10^6 K. The main source of EUV radiation is the transition region between the chromosphere and corona.

Soft X-ray emission is between 0.1 nm and 10 nm.

Hard X-rays are below 1 nm.

X-ray emission is highly variable

Soft X-ray from GOES satellite (last 2 days)



Updated 2015 Sep 9 14:09:13 UTC

NOAA/SWPC Boulder, CO USA

Real-time solar images

<http://jsoc.stanford.edu/data/hmi/images/latest/>

<http://sdowwww.lmsal.com/suntoday/>

<http://heliviewer.org/>

<http://www.bbso.njit.edu/cgi-bin/LatestImages>

<http://sohowww.nascom.nasa.gov/>

<http://www.raben.com/maps/>